Recent developments and trends in miniaturized gas preconcentrators for portable gas chromatography systems: A review

Irene Lara-Ibeas, Alberto Rodríguez Cuevas, Stéphane Le Calvé

RECENT DEVELOPMENTS AND TRENDS IN MINIATURIZED GAS PRECONCENTRATORS FOR PORTABLE GAS CHROMATOGRAPHY SYSTEMS: A REVIEW

Irene Lara-Ibeas[1], Alberto Rodríguez Cuevas[1,2], Stéphane Le Calvé[1]*

[1] Institut de Chimie et Procédé pour l'Energie, l'Environnement et la Santé (ICPEES, UMR 7515 CNRS/Unistra), group of atmospheric physical chemistry, 25 rue Becquerel, 67087 Strasbourg Cedex 02, France.

[2] In'Air Solutions, 25 rue Becquerel, 67000 Strasbourg, France.

Abstract

In the last years, a growing number of fields such as air quality monitoring, breath analysis or explosives and chemical warfare agents detection requiring fast, on-site, sensitive analysis has led to the development of portable gas chromatography systems. In most cases, these systems integrate a miniaturized gas preconcentrator, which provides a significant enhancement of the sensitivity enabling quantification of analytes present in the sample at trace levels. In this review, the authors have focused on recent developments in these preconcentrators integrated in portable gas chromatography systems. The main materials and fabrication techniques, designs, heating technologies, fluidic connections, adsorbents, and applications are discussed. In addition, an analysis of some factors affecting preconcentration performance is presented. A new figure of merit called Normalized Preconcentration Efficacy (NPE) is proposed to evaluate the performance of these devices in a standardized manner, making possible a more straightforward comparison between different devices.

Keywords: Preconcentration, Miniaturization, Microfabrication, Gas chromatography, VOC detection, Normalized Preconcentration Efficacy (NPE)

1. Introduction

Gas chromatography (GC) has been largely used in the detection of volatile organic compounds (VOC) for decades. The versatility of this technique lies in the broad spectrum of detectors and separation columns that can be combined resulting in analytical instruments suitable for many applications such as

explosives detection [1,2], air quality monitoring [3,4], occupational exposure [5,6] or breath analysis [7,8], among others.

Traditional GC benchtop instruments uses capillary columns coated with stationary phases of different polarity to separate the analytes of interest. These columns are coupled to very sensitive detection systems like mass spectrometers (MS) or flame ionization detectors (FID) which enable to identify and/or quantify a great number of chemicals. In these systems, preconcentrators (PC) are usually located upstream the separation column and have two main functions: to narrow the chromatographic band and to improve the detection limit. In benchtop instruments, PCs, also called cold traps, are usually kept sporadically at sub-zero temperatures to promote the adsorption of analytes. After trapping the analytes, the sample is subsequently heated, and a flow of inert gas is employed to transfer the analytes into the separation column. Temperatures of 150–350°C are reached in few seconds in a process called flash desorption which ensures the total desorption of analytes and their transfer to the column in a very sharp band. This technique is very efficient to produce narrow chromatographic peaks and consequently produces a significantly increase of sensitivity, being able to detect chemicals at concentrations in the order of parts per billion (ppb) or parts per trillion (ppt) when coupled to MS or FID. However, these instruments are very bulky and require high power supply, limiting their use for on-site applications.

In the last decades, the implementation of stricter environmental laws, especially in Europe [9] and the increasing demand of applications requiring rapid responses to specific events such as chemical warfare agents or explosive detection has led researchers to develop portable gas chromatographs to perform on-site analysis. Although many efforts have been performed since then, the main challenges of portable instruments lie in keeping similar performances to benchtop instruments while the size and the energy consumption are drastically reduced. However, in some cases, these performances are still far from the ones of their benchtop counterparts, especially in terms of sensitivity, since the detection limits of portable GC are usually in the order of 10 – 10,000 ppb whereas the benchtop instruments can very often detect concentrations of less than 1 ppb (typically 0.01 – 1 ppb).

Due to their low power consumption and reduced size, compact detectors such as mini photoionization detectors (miniPID) [4,10,11], thermal conductivity detector (TCD) [12], metal oxide (MOX) sensors

[8,13] and chemiresistors (CR) [6] are typically employed in portable gas chromatography (see Table 1 and Table 2). Nevertheless, their sensitivity without any previous preconcentration step varies from ppb (miniPID) to ppm levels in most of them. Therefore, preconcentrators (PC) become a key component in portable GC to reach limits of detection (LOD) at sub ppb levels.

During operation, PCs must be rapidly heated to release the trapped analytes in a narrow chromatographic peak as abovementioned which requires high power supply. However, portable instruments have limited power supply, therefore, the thermal mass of PC must be reduced. Other issue arising from the operation of PC in portable devices is the thermal isolation of the PC to avoid heat losses and prevent the damaging of surrounding components. Microfabrication techniques allow to create devices with reduced thermal mass and integrated powerful heating systems [14,15]. However, the problems related to the fluidic interfacing and the need for cleanrooms for their development has brought researchers to adopt new approaches for PC miniaturization. Recently, 3D printing [16] or milling [4] have been employed as alternative fabrication techniques in the fabrication of miniaturized PC. At present, these techniques do not have the features to create microstructures with the same accuracy as microfabrication techniques, but they enable easier fluidic interfacing and may reduce the costs of the prototyping process.

Table 1. Portable GC coupled to photoionization detectors (PID) with integrated PC and their features.

Ref.	Size (cm^3)	Weight (kg)	Analysis time (min)	Sample Volume (mL)	Preconcentrator					Target compounds	Det.	LOD (ppb)	Sensitivity (pg)
					l **(mm) × *d* (μm) × *w* (mm)**	**Material**	**Adsorbent**	**Heating system**	**Power cons. (W) / heating rate (°C/s)**				
GC-PID [4]	32 × 29 × 14	~ 5	19	20	Cavity (4.6 × 350 × 7.4)	Al	C-B 5 mg	Ceramic heaters	~ 44 / 4.8	BTEX	PID	0.06 – 0.4 (BTEX)	3.6 [a]
GC-PID [17]	35 × 26 × 15	< 5	5	90	Tube (4 mm i.d., 40 mm length)	Glass	CNT sponge 5 mg	CNT sponge	n. a. / 450	BTEX	PID	0.13-0.28 (BTEX)	37.4 [a]
MAP [10]	32 × 29 × 14	~ 5	19	20	Manifold-shaped cavity 4.6 × 350 × 7.4	Al	Basolite C300 5.8 mg	Heating cartridges	210 / 2.5	BTEX	PID	0.1-1.6 (BTEX)	6.4 [a]
GC-PID [18]	31 × 30 × 20	32	~35	4000	Tube 0.165 cm i.d.	n. a.[g]	ResSil-B 75 mg	n. a.	n. a.	34 VOC	PID	0.002 - 0.011 (BTEX)	140.6 [a]
GC-PID [19]	n. a.	n. a.	6	n. a.	4 Parallel channels n.a. × 400 × 0.6 μm	Si-glass	SWNTs 0.15 mg	Cr/Pt	n. a.	5 VOC	PID	< 1 [a]	n. a. [a]
Frog 4000 [11]	25 × 19 × 37	< 2.2	5.5	n. a.	n. a.	Si-glass	Silica gel aerogel	n. a.	n. a.	n. a.	PID	~ ppb	n. a. [a]
GC-PID [20]	n. a.	n. a.	63	600	Parallel channels 25 × 1.3 mm × 12	Si-glass	EtQxBox 10 mg	Pt	n. a. / 50	Benzene	PID	1.25 [a]	2396 [a]
GC-PID [15]	60 × 50 × 10	< 5	16.2	50	Tapered cavity 8.15 × 250 × 2.9	Si-glass	C-B 1.135 mg	Pt	n. a. / 314	50 VOC	μPID	n. a.	n. a.
GC-PID [21]	30 × 17 × 8	< 3	15	1000	Tube 1.2 mm (i.d.) × 8 cm (l)	Stainless Steel	C-B 3 mg C-X 2 mg C1000 1 mg	NiCr wire	n. a. / 75	10 VOC	PID	0.02[a] -0.36	90[a]-1051

l: length, d: depth, w: width; Power cons.: power consumption; Det.: Detector; LOD: Limit of Detection, i.d.: inner diameter; n.a.: not available; CNT: carbon nanotubes; PID: photoionization detector; C-B: Carbopack B; C-X: Carbopack X; C1000: Carboxen 1000; [a] value given for benzene.

Table 2. Portable GC coupled to different detectors other than PID with integrated PC and their features.

Ref.	Size (cm^3)	Weight (kg)	Analysis time (min)	Sample Volume (mL)	Preconcentrator					Target compounds	Det.	LOD (ppb)	Sensitivity (pg)
					l (mm) × *d* (µm) × *w* (mm)	Material	Adsorbent	Heating system	Power cons. (W) / heating rate (°C/s)				
PEMM-2 [6]	20 × 15 × 9	~2.1	3	5	2 Cavities (V~4.7 µL)	Si-glass	C-B 2.0 mg C-X 2.3 mg	Ti/Pt	1 / -	9 VOC	µCR array	16−600 (150 [a])	2396 [a]
Ceramic PC [22]	-	-	~50	200	Manifold shaped cavity 61 × 5.5 mm × 23 mm	Ceramic	C-SII 1.187 g	Tungsten	18 / 0.25	Ethylene	EC	25	5736
GC-MOS [8]	n. a.	n. a.	9	250	Cavity with micro-pillars 10 × 400 × 5	Si-glass	Zeolite DaY ~13 µm	-	-	4 VOC	MOS	24 [b]	22611 [b]
GC-CMOS [23]	16 × 11 × 11	n. a.	n. a.	-	Cavity with micro-pillars 10 × 250 × 2	Si-glass	Carbon film	Ni-Cr wire	-	7 VOC	CMOS	15 (1,3,5-TMB)	-
iGC3.2 [24]	8 × 10	n. a.	130	24	U shape n.a. × 300 × 1350	Glass	C-B + C-X	Ti/Pt	10.5 / 46	19 VOC	2 CD	10 – 2 (BTEX)	766.7 [a]
Zebra GC [12]	15 × 30 × 10	~1.8	< 12	10	Cavity with micro-pillars 13 × 240 × 13	Si-glass	Tenax TA ~200 nm	Cr/Ni	16 / 25	6 VOC	TCD	~25 (TEX)	942.1 [a]
INTREPID [2]	33 × 29 × 13	5.4	2	1000	Tapered cavity 3.2 mm (l) × 3.5 mm	Si-glass	C−B 2.4 mg	Gold	- / 75	2,4-DNT, 2,3-DMNB, 2,6-DNT	µCR array	0.067-0.30	500-2200
GC-MOS [25]	-	-	3	100	Planar Microhotplate 1.2 µm thick SiO_2/Si_3N_4 dielectric layer 2 × 4.5	SiO_2/Si_3N_4	Activated Carbon	Pt	1.02 µW/ºC	Benzene	MOS	< 1000 [a]	-
GC-MOX [13]	n. a.	n. a.	~67	2750	Ten parallel channels 800 µm depth	Si-glass	QxCav	Pt	- / 50	Benzene	MOS	0.1	878.5 [a]

l: length, d: depth, w: width; Power cons.: power consumption; Det.: Detector; LOD: Limit of Detection, i.d.: inner diameter; n.a.: not available; C-B: Carbopack B; C-X Carbopack X, C1000: Carboxen 1000; CR: chemiresistor; TCD: thermal conductivity detector; MOS: Metal Oxide Semiconductor; CD: Capacitive Detector. CMOS: Complementary Metal Oxide Sensor. MOX: Metal Oxide sensor. QxCav: Quinoxaline bridged Cavitand; EC: electrochemical sensor; n.a.: not available; [a] value given for benzene; [b] value given for toluene.

Another way to reduce the power consumption is by optimizing the adsorption-desorption process. Therefore, recent efforts of some research groups have been focused on developing foam-based adsorbents that present lower pressure drop and more efficient heat transfer than conventional adsorbents while maintaining a reasonable adsorption capacity. Various types of gas micro preconcentrators and their main parameters and features are presented in Table 3 and Table 4.

Researchers working on the development of preconcentrators are often specialists from very different fields, namely microfluidics, electronics, material science, analytical chemistry, or air quality. Given this variety of approaches, different measurement units are used to quantify the same magnitudes: ppb and $\mu g\ m^{-3}$ for gas concentrations, or even in mass unit (ng or pg) of analytes injected into the analytical instrument. This diversity makes comparisons of analytical performances between different systems very difficult, especially when different chemicals are tested. Moreover, a preconcentrator, by definition, concentrates the gas sample for a given time to achieve a certain sensitivity. Thus, the sample volume and the time-resolution are parameters to be considered in the evaluation of portable chromatographs. The present review article covers the last trends in the development of miniaturized preconcentrators for portable gas chromatography. A general overview of gas preconcentration followed by thermal desorption is presented in Section 2; the recent developments in these preconcentrators which includes materials and fabrication techniques, design, heating technologies and fluidic interfacing, adsorbents and applications are reported in Section 3. Additionally, in this section, a comparison of the preconcentration performance of different devices and guidelines to evaluate this performance in a normalized manner are provided. Conclusions are presented in Section 4.

Table 3. Preconcentrators packed with commercial granular adsorbents.

Ref.	Target compounds	Adsorbents	PC Microstructure and dimensions *l* (mm) × *d* (µm) × *w* (mm)	Materials	Heating system	Power cons. (W) / Heating rate (°C s^{-1})	Det. & LOD (ppb)	PF	Sample volume	Application field
[26]	SVOC and VOC	C-X 780µg C-B 830 µg	Two concentric rings of apertures (8 × 8 mm whole chip)	Si-glass	Pt	2 / 150 - 400	n. a.	n. a.	n. a.	Environmental monitoring, CWA detection
[27]	BTEX	Tenax TA	Tapered cavity 21 mm (l) × 400 µm (d) × 7.6 mm (w)	Si-glass	Pt	n. a. / 19	MS	n. a.	n. a.	Breath analysis
[28]	Isoprene	C-X 20 mg	Manifold with 4 µchannels 12.6 x 2.5 mm x 16	Copper	Ceramic heater	10.14 / 5.5	FID	352[n]	18	Breath analysis
[20]	BTEX	EtQxBox 10 mg	Parallel channels 25 mm (l) × 1.3 mm (d) × 12 mm (w)	Si-glass	Pt	n. a. / 50	PID 1.25 [b]	-		Environmental monitoring
[29]	12 VOC	Tenax TA ~7 mg	Square cavity 2.54 cm (l) × 2.54 cm (d) (chip)	Glass	2.8 / 17.6	n. a.	FID 22	5.1-10.3[a]	n. a.	-
[30]	Ethylene	CBS-II 191.0 mg	8 parallel channels 40.0 mm (l) × 0.9 mm (d) × 2.0 mm (w)	Glass-Si-Glass	Tungsten	n. a.	EC 3.8	7.7[b]	220	Food industry
[7]	Acetone	CBX 1012 ~ 4 mg	Spiral microchannel 120 mm (l) × 0.35 mm (d) × 0.35 mm (w)	Si-glass	Pt	4.52 / n. a.	GS 800	2500[c]		Breath analysis
		CBX 1018 0.95 - 11.3 mg	Tube 0.2 mm (i.d.) × 0.4 mm (o.d.) × 46.8 mm (l)	Glass	Ni-Cr wire	8.57 / n. a.	GS	~ 800 [c]	3000	Breath analysis
		CBX 1018 0.95 - 11.3 mg	Tube 0.7 mm (i.d.) × 1.2 mm (o.d.) × 38.2 mm (l)	S.S	Ni-Cr wire	17.67 / n. a.	GS	~550 [c]		Breath analysis
[31]	Benzene	HKUST-1 ~ 30 mg	Hotplate 3 mm (l) × 3 mm (w)	Alumina	Alumina	0.43 / n. a.	MOX	10[n]		Environmental monitoring
[32]	4 VOC	CB + Tenax	Tubular rolled plate 2 mm (l) x 1 mm (i. d.)	Polyimide	Gold	1.7 / 40	PID	8-200[c]	2000	Explosives detection
[5]	17 VOC	C-X 1.4 mg C-B 2.0 mg	2 tapered cavities 380 µm deep	Si-glass	Pt	n. a. / n. a.	FID	620[d]	31	Occupational exposure
[1]	ONT	Zeolite DaY 2.25 mg	Rectangular cavity with pillars 5 mm (l) × 400 mm (d) × 10 mm (w)	Si-glass	Pt	n. a. / n. a.	MOX 365	7.2[e]	500	Explosives detection
[33]	TCE	C-X ~2.3 mg	Tapered cavity 3.2 mm (l) × 3.5 mm (w)	Si-glass	Pt	n. a. / 375	ECD 1.2	800000[d]	20000	Environmental monitoring
[16]	Toluene	HayeSep D 119.9 mg	Tube with micro-pillars 38.68 (l) × 7.69 mm (o.d.)	Stainless steel	NiCr wire	14.6 / 1.8	MS	n. a.	180	Environmental monitoring

l: length, d: depth, w: width; Power cons.: power consumption; Det.: Detector; LOD: Limit of Detection, i.d.: inner diameter; o.d.: outer diameter; n.a.: not available; C-B: Carbopack B; C-X Carbopack X, CBX: Carboxen; GS: gas sensor; MOX: Metal Oxide sensor; ECD: electrochemical detector; n.a.: not available; Method employed for the calculation of the preconcentration factor: [a] ratio of the concentration peak area of the PC packed with adsorbent to that of the PC without adsorbent, [b] ratio between peak area of the detector with and without the presence of a PC, [c] ratio between the maximum concentration measured at the desorption step and the initial concentration of the injected sample gas, [d] ratio of the volume of the air sample collected to the volume in which that same mass is contained at the point of detection, [n] not mentioned.

Table 4. Preconcentrators filled with thin film and foam adsorbents.

Ref.	Target compounds	Adsorbents	PC Microstructure and dimensions *l* (mm) × *d* (μm) × *w* (mm)	Materials	Heating system	Power cons. (W) / Heating rate (°C s^{-1})	Det. & LOD (ppb)	PF	Sample volume (mL)	Application field
[34]	BTEX	MOF foam 85 mm^3	11 × 100 × 8 Square cavity	Si-glass	Pt	4.2 / 22	FID	144[c]	50	Environmental monitoring
[35]	BA, EB,p-X	Tenax-TA	Cavity filled with U-shaped micropillar array	Si-glass	n. a.	n. a.	FID	n. a.	n. a.	-
[36]	Ethane	CNT Foam	Rectangular cavity 13 mm (l) x 1.5 mm (d) x 11 mm (w)	Si-glass	Pt	4.8 / 25	FID	90.2[b]	150	Breath analysis
[37]	Benzene, toluene, styrene	SWCNT 0.15 mg	Four parallel channels of 350 μm (d) 10 mm (l) with micropillars	Si-glass	n. a.	n. a.	PID	n. a.	n. a.	Environmental monitoring
[38]	Toluene, m-xylene	Tenax-TA ~3.7 μm	Tapered cavity with cylindrical micropillars 9 mm (l) × 400 mm (d) × 5 mm (w)	Si-glass	Gold	n. a. / 75	FID	7900 // 14800[a]	150	-
[39]	Hexane	Silicalite 1 4.4 mg	Tapered cavity (A) ~54.0 mm (l) × 10 mm (w)	Si-glass	Gold	8 / n. a.	MS	48.9 ± 10.4[c]	50	Occupational exposure
		Silicalite 1 4.1 mg	Tapered cavity (B) ~54.0 mm (l) × 10 mm (w)			8 / n. a.		42.6 ± 15.3 [c]		
		Silicalite 1 4.6 mg	Tapered cavity with square pillars (C) ~54.0 mm (l) × 10 mm (w)			8 / n. a.		13.7 ± 2.5 [c]		
		Silicalite 1 4.7 mg	Tapered cavity with pillars (D) ~54.0 mm (l) × 10 mm (w)			8 / n. a.		30.9 ± 1.2 [c]		
[40]	Benzene	SWCNTs (0.15 mg)	4 microchannels 400 μm (d) × 1000 μm (w)	Si-glass	Pt	n. a. / 3.5	PID	n. a.	150	Environmental monitoring

l: length, d: depth, w: width; Power cons.: power consumption; Det.: Detector; LOD: Limit of Detection, n.a.: not available; n.a.: not available; Method employed for the calculation of the preconcentration factor: [a] ratio of the concentration peak area of the PC packed with adsorbent to that of the PC without adsorbent, [b] ratio between peak area of the detector with and without the presence of a PC, [c] ratio between the maximum concentration measured at the desorption step and the initial concentration of the injected sample gas, [d] ratio of the volume of the air sample collected to the volume in which that same mass is contained at the point of detection, [n] not mentioned.

2. General overview of gas preconcentration followed by thermal desorption

In gas preconcentration devices, a cavity is packed or coated with an adsorbent to capture the molecules of interest. The working principle of preconcentrators (PC) is based on the adsorption of these molecules on the adsorbent followed by a fast thermal desorption (see Figure 1). In the first step, the analytes are collected on an adsorbent either by active flow [41,42] or through passive exposure [43,44]. In active flow sampling, the adsorbent is contained in an enclosed space and a specific sample volume is passed through the adsorbent bed by means of a pump. In this type of sampling, since all the sample volume pass through the adsorbent, a complete trapping of the analytes present in the sample is expected. Due the power requirement of the pumps, active sampling is used in applications where gas concentrations must be measured for short periods of time (typically minutes to hours) [43]. In passive sampling, adsorbents are usually exposed to the sampled medium, i.e., usually indoor or outdoor air, and the theoretical volume of sampling air is determined according to the gaseous diffusion rate of each analyte in the investigated media. Passive sampling is commonly used to monitor gas concentrations during long time periods ranging from some days up to several weeks [43,45].

In active as well as passive sampling, the analytes collection is typically conducted at room temperature [41], and sporadically at sub-zero temperatures [40] to enhance the adsorption of analytes. Once the adsorption is completed, the preconcentrator is rapidly heated to relatively high temperatures, i.e., in the wide range 150 – 350 °C and more usually between 250 and 300 °C. This temperature increase results in the desorption of the analytes into a much smaller volume compared to the original sample, thus increasing their concentration prior to the analysis. Furthermore, this rapid increase leads to the injection of analytes in the column in the form of a narrow plug, increasing sensitivity. That is the reason why in some studies, PC are also referred to as preconcentrator-injector (PCI) or preconcetrator-focuser (PCF) [5,33,46,47].

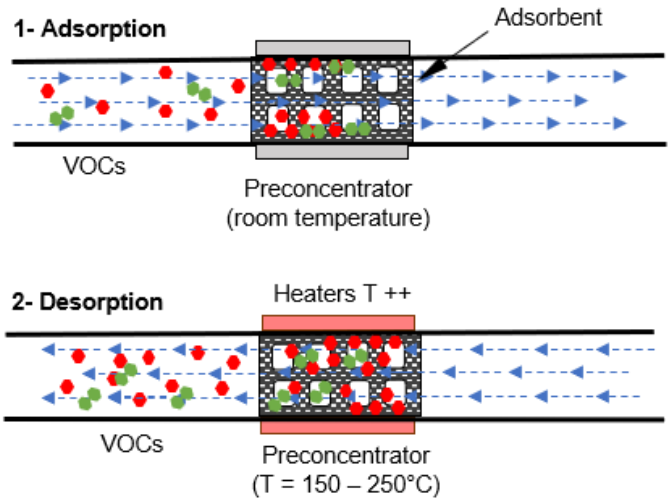

Figure 1. Schematic representation of the adsorption and thermal desorption of VOCs.

As mentioned above, the preconcentration process consists of two consecutive steps, adsorption and desorption. The efficiency of the whole process is determined by several factors affecting these two stages:

- The physico-chemical properties of the adsorbent. Thermal stability, surface area and polarity of the adsorbent dictate the long-term efficiency, maximum adsorption capacity, and strength and nature of adsorbate-adsorbent interactions. Relatively strong interactions are required between the analytes and the adsorbent to capture the analytes at room temperature; however, this process should be reverted when temperature increases. Chemisorption is not desired since this process may involve changes in the chemical structure of the analytes.
- The experimental conditions employed. Temperature, sample volume, and analyte concentration during the adsorption step determine the total amount of analyte trapped. During the desorption step, the carrier gas flow rate, desorption temperature and heating rate condition the desorption efficiency and the narrowness of the chromatographic peaks.
- Preconcentrator design and configuration of the experimental setup. Geometry of the preconcentrator cavity influences the residence time of the sample and, therefore, the probability of the analytes to be captured. Dead volumes in the fluidic path of the system may contribute to the dilution of the sample prior to the analysis, thus reducing the efficiency of the

preconcentration process. Similarly, this kind of flow path disruptions tend to generate peak tailing in the chromatograms. In addition, the materials employed in PC fabrication determine the heat transfer and therefore the desorption rate.

3. Recent developments and trends in miniaturized gas preconcentrators

Because of the high demand of sensitive and portable analytical instruments, several miniaturized gas preconcentrators have been developed over the years. Miniaturized preconcentrators can be defined as device which serve to increase the analyte concentration in a sample and whose fluidic path have dimensions of microns implying the use of microfabrication techniques. The size of these devices can go from few millimetres up to 10 mm whereas their weight can reach up to few tens of grams. Some examples are displayed in Figure 2. While the working principle of the PC remains the same, new developments including designs, materials, fabrication techniques, or adsorbents have been recently proposed. These developments are reviewed in detail in this section and their main characteristics, performances and future challenges are presented.

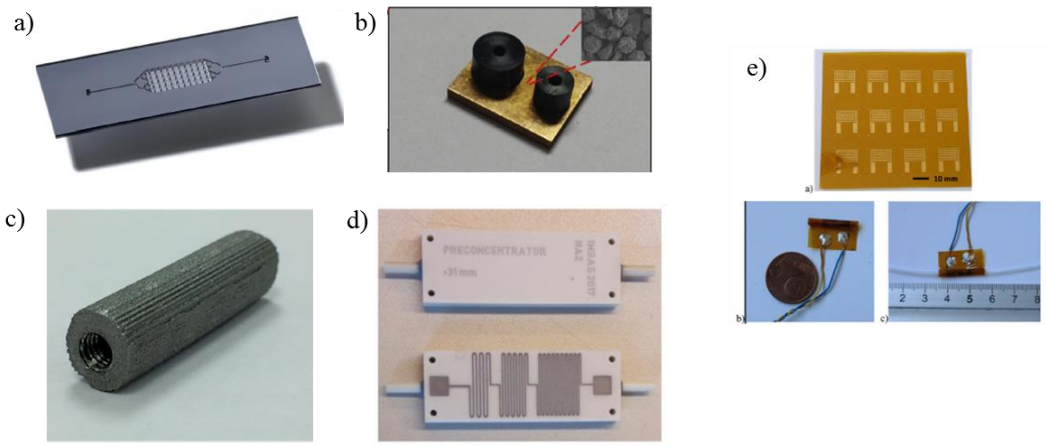

Figure 2. Micro preconcentrators made of diverse materials: (a) silicon-glass (microcavity dimensions: 5 mm wide, 10 mm long and 400 µm deep) [8], (b) cooper (device dimensions: 16 mm long, 12.6 mm wide and 2.5 mm deep) [28], (c) stainless steel (tube dimensions: 38.68 mm long and 7.69 mm of outer diameter) [16], (d) ceramics (device dimensions: 61 mm long, 23 mm wide and 5.5 mm deep) [22] and (e) polyimide foil (tube dimensions: 2 mm long and 1 mm of internal diameter) [32].

3.1. Materials and fabrication techniques

Several materials have been employed for the fabrication of miniaturized gas PCs. PCs are subjected to continuous temperature cycles that conditions the selection of these materials. Ideally, the material

employed for the fabrication of a PC should be thermally resistant to preserve its structure after several adsorption-desorption cycles which involve rapid heating and cooling. Furthermore, an effective heat transfer from the heaters to the adsorbent is desired to promote the fast desorption of analytes. Therefore, a low heat capacity and a minimal thermal mass are paramount to allow a fast temperature ramp.

In this regard, silicon or glass-based PCs machined by MEMS (Micro-Electro-Mechanical Systems) techniques are advantageous due to their reduced thermal mass and, therefore, power consumption. However, the multiple cleanroom-based processes which can be expensive or time-consuming altogether with the high level of research and development required to get a successful device, has led several research groups to develop miniaturized PCs using alternative materials and fabrication techniques.

The main advantage of these recently developed devices lies in the possibility to be manufactured in research laboratories without cleanroom requirements making the fabrication process more accessible and, in most cases, reducing time and costs. Furthermore, standard fluidic connections assuring gas tightness are usually easy to integrate in these devices due to their larger dimensions compared to those of MEMS-based devices. However, these dimensions involve higher thermal mass, resulting often in higher power requirements and slower temperature ramps.

3.1.1. Silicon

In the last decades, MEMS technology has been widely used for the fabrication of PCs [1,5,20,26,27,33–40]; therefore, most of these devices are made of materials related to the electronics industry. So far, silicon has been the most employed material due to its relatively high thermal conductivity and the variety of existing micromachining techniques. A typical preconcentrator made of silicon is illustrated in Figure 2a. This material provides low thermal mass, uniform thermal distribution, and the ability to handle high temperature ramping rates [48], the most relevant features in miniaturized preconcentrators.

Silicon micromachining is generally conducted at cleanroom facilities by wet or dry etching. Wet etching techniques involve the use of liquid chemicals such as hydrofluoric acid or potassium hydroxide to remove the exposed surfaces of the substrate. These techniques played an important role in the early

stages of MEMS development to create microfluidic cavities and channels in silicon at a relatively low cost compared to other etching techniques [29,39]. Wet chemical etching is isotropic and produces rounded side wall microchannels. The depth of the these channels is controlled by the etch rate and etch duration whereas the width of the microchannel can be estimated by the mask opening plus twice the channel depth [49]. Therefore, high aspect ratio features are hard to build using these methods. For that reason, their use in PC fabrication has been limited [39]. On the contrary, dry etching techniques offers the possibility to create high aspect ratio structures. In this process, etching is conducted by ions that collide and react with the exposed surface of the silicon wafer instead of using liquid chemicals [48]. The most widespread technique for creating cavities, channels, and pillars with different geometries in silicon-based PC is the deep reactive ion etching (DRIE). DRIE allows to create nearly vertical sidewalls of high surface quality in silicon. For example, using this technique, microchannels 250 µm deep and 25 µm wide have been etched to create gas chromatography microcolumns [50]. Once the cavities are etched, the substrate is bonded to another plate usually made of glass resulting in a sealed chip. Anodic bonding is the most common technique for silicon-glass bonding [6–8,19,34,36,37,51–53]. In this process, a DC voltage ranging from 500 to 2000 V is applied between the substrates whereas they are heated to temperatures varying from 300 to 600 °C [48]. The generated electric field leads to the migration of Na^+ ions from the silicon/glass interface, leaving oxygen ions (O^{2-}). These ions react to form a layer of siloxane (Si-O-Si) ensuring the irreversible bonding between the substrates [54,55]. As can be seen in Table 3 and Table 4, more than 70% of PCs developed in the last years are silicon-glass hybrid devices. In these devices, the heating system can be easily integrated by patterning a metal layer (typically Pt or Au) on the silicon substrate.

3.1.2. Glass

Although silicon-glass hybrid PCs are the most common, some devices have been fabricated entirely from glass. McCartney et *al*. [29] developed a robust micro gas PC made of glass (Borofloat 33 by Schott Co.). In this device, the cavity was created by wet etching using 49% hydrofluoric acid solution. Unlike DRIE, some steps of this wet etching procedure can be conducted outside of a cleanroom. The heating system and temperature sensors were created with a photolithography-free technique enabled

by laser etching. To seal the chip, the glass die containing the microcavity was bonded to another glass die by thermal fusion bonding.

Qin and Gianchadani [24] developed a fully microfabricated gas chromatograph in which all the components were fabricated using glass dies. In this device, the metallization and micromachining were performed on separate glass substrates. The microchannels and ports for fluidic connections were created by sandblasting. This process enables to create high aspect ratio structures and quickly remove large areas of material being suitable for the creation of deep channels as well as through-holes. In the case of the PC, the metallized and the micromachined glass dies were bonded by adhesive bonding using Epotek-377 epoxy, followed by baking at 300 °C for >1 h to minimize outgassing during operation. This technique is a simple, robust, and low-cost bonding procedure that, in addition, do not require a cleanroom to be performed.

3.1.3. Metal

The well-known drawback of most of silicon and glass micromachining techniques is mainly the need for cleanroom facilities. Furthermore, even though these fabrication processes are well established, PCs made of these materials are very fragile and failures are frequent during the fabrication and the assembly process. Laser etching technology, milling or metal 3D printing techniques have been recently employed as alternative techniques for the fabrication of miniaturized PCs. The late improvements in these techniques provide the possibility to fabricate miniaturized PCs made of more robust materials at a low cost. Han et *al*. [28] fabricated a micro metal gas preconcentrator (MGP) made of copper (C11000) for the detection of isoprene (see Figure 2b). This material has a thermal conductivity about 2.6 times higher than that of silicon, and a specific heat capacity of about a half of that of silicon promoting temperature uniformity along the chip. Furthermore, copper (C11000) has good chemical stability, can be micromachined by traditional manufacturing methods and is much more robust than silicon or glass. The MGC layout consist of 4 microchannels (each is 1 mm width, 3 mm long and 500 μm depth), and two symmetrical manifold fluidic systems etched in a C11000 substrate by laser etching technology (LET). This substrate was bonded using of vacuum diffusion welding (VDW) to another copper plate in which inlet and outlet ports were etched.

Huang et *al*. [16] printed a stainless steel PC using jet binder printing (BJP) technique (see Figure 2c). In this additive technique, the parts are built by spreading the printing powder in a layer-by-layer fashion. After the printing process, the device must be heated in an oven, first at 195°C for 2h for the binder phase to cure and then, at 460°C for 2h for the decomposition of the remaining binder phase. Finally, the device is sintered in a high-vacuum oven at 1250°C for 6 h. To minimize the porosity of the printed parts, sintering additives such as boron nitride (BN) were added to the stainless-steel powder used for the printing. BJP technique allows to manufacture devices with submillimeter internal features that can operate at high temperatures. A standard 10-32 port thread was machined to connect commercial compression fittings resulting in a gas tight connection and facilitating its integration into the GC system.

Aluminium has been also used in the manufacture of miniaturized PCs. Lara-Ibeas et *al*. [10] proposed a PC made of aluminium for the detection of BTEX. In this device, the microfluidic cavity and two symmetrical manifolds were machined on an aluminium substrate by traditional precise milling methods. Two porous metal filters were integrated at both sides of the cavity to retain the adsorbent. The device was covered with another aluminium plate and the sealing was assured by four screws and a Viton gasket. Rodriguez-Cuevas et *al*. [4] manufactured a micro gas PC made of aluminium in their research lab using also precision milling. The device consisted of an aluminium block with two lateral tubes. Custom-made PEEK reducing unions were inserted in these tubes resulting in reliable gas-tight connection to the GC system.

3.1.4. Other materials

Other materials have been employed in the fabrication of miniaturized PCs but to a much lesser extent. Zaidi et *al*. [56] developed a micro preconcentrator made of aluminum nitride ceramics (see Figure 2d) for the detection of ethylene. The chip was manufactured using ceramic technology and the two parts were bonded by co-firing. Unlike other microdevices, this PC can be easily integrated in the chromatographic system due to the two cylindrical hoses glued to the PC for the gas inlet and outlet. Camara et *al*. [32] reported the use of polyimide foil for the fabrication of a PC (see Figure 2e). The main advantages of using this material are low-cost and easy processing. Additionally, this PC are

flexible, and the diameter of the inlet/outlet can be adjusted to work at higher flow rates than in their silicon counterparts, reaching up to 1.5 L/min.

3.2. Design and microstructures

The main microstructures reported in the literature can be divided in two types: planar hotplate and three dimensional (3D) structures. Planar hotplates consisted of a planar substrate coated with an adsorbent selective to the target molecules [57]. This design is much easy to fabricate and offers a low power consumption, however, owing to its configuration, the amount of adsorbent that can be hosted in these devices is limited, which reduces the adsorption capacity and, therefore, their preconcentration performance. This major drawback has led to a change of trend in PC design which has shifted progressively from planar to 3D preconcentrators. In the last decade, only few planar preconcentrators have been reported in the literature. Lahlou et *al*. [25] developed a planar micropreconcentrator-injector for the detection of benzene. This device consisted of a planar rectangular membrane of a 1.2 µm thick SiO_2/Si_3N_4 dielectric layer, which was suspended on a silicon substrate. An activated carbon layer was deposited on the membrane by drop-coating and used as adsorbent. Leidinger et *al*. [31] used alumina microhotplates to fabricate a planar micropreconcentrator for air quality monitoring. Two metal-organic frameworks (MOF), HKUST-1 and MIL-53, were deposited on the hotplates by drop coating and their preconcentration efficiency was evaluated for benzene and toluene.

Currently, most of micro-PCs present a 3D structure. This configuration offers a higher collection capability since the amount of adsorbent packed is greater than in the case of planar PCs. Nonetheless, several aspects must be considered to ensure good performance of these devices:

- Uniform flow distribution inside the device to optimize the adsorption through the whole adsorbent bed;
- Low pressure drops to limit the risk of gas leaks and decrease operation costs due to high pressure in the microdevices;
- Large contact surface and long contact time between the adsorbate and the adsorbent to increase the probability of the molecules to be adsorbed and trapped;

- Efficient and fast heating but also uniform heat distribution.

Taken into account these aspects, several 3D PCs with a variety of geometries have been proposed in the literature such as circular spiral [58], array of parallel channels [28] or single U-shaped channel [24] (see Figure 3).

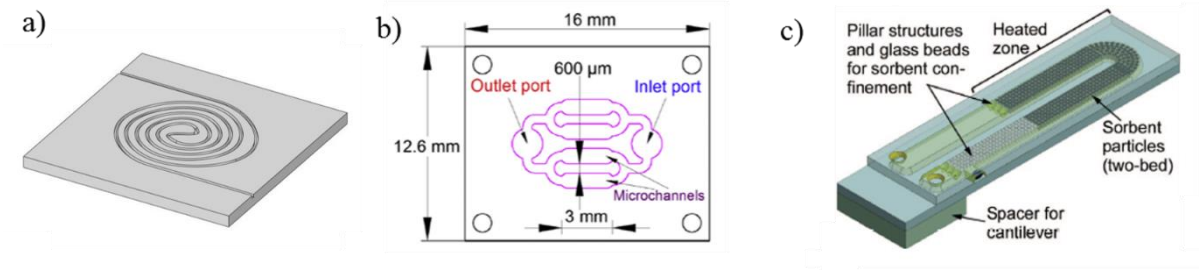

Figure 3. Preconcentrators with different geometries: circular spiral (a) [58], array of parallel channels (b) [28] and U-shape cannel (c) [24].

Due to the narrowness of the microchannels altogether with the flow resistance added by the adsorbent particles, some of the one-single channel designs often shows relatively high pressure drops. Therefore, designs leading to lower pressure drop, such as a wide rectangular cavity connected to inlet and outlet channels [6,10,22,39] are usually preferred. In these microdevices, prior to fabrication, flow simulations are frequently conducted to estimate the pressure drop and optimize the distribution of the gas flow. Li et *al*. [59] performed computational fluid dynamics (CFD) simulations and demonstrated the influence of the inlet angle on the flow field near the inlet (see Figure 4a). They reported that uniform gas flow velocity distribution can be achieved when the triangular angles in the inlet and outlet are smaller than 120°. Hence, as can be inferred from Table 1 and Table 2, it is very common to observe tapered cavities in micro PCs [8,10,23,28,38,56] as illustrated in Figure 4b.

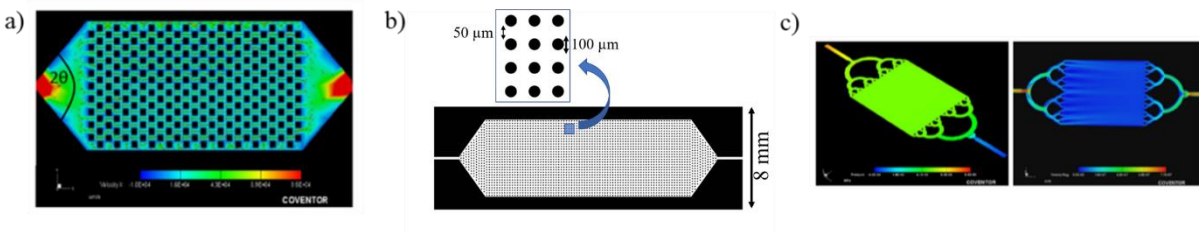

Figure 4. (a) Flow simulation in a PC with inlet/outlet angle > 120 ° [59]; (b) Preconcentrator containing micropillars and having inlet and outlet angles > 120 ° [23]; (c) Pressure (green) and flow velocity (blue) simulations in a PC with inlet/outlet manifold fluidic system [60].

To create a more uniform flow distribution, some authors have added symmetrical manifolds at both sides of the main cavity where the adsorbent is packed [10,60] (see Figure 4c). These manifolds split the inlet flow in several channels thus promoting uniformity of the gas flow through the adsorbent bed.

In a PC loaded with granular adsorbents, the cavity is usually flat although, in some cases, microstructures have been also included to improve the flow distribution without significant reductions in the amount of adsorbent that can be hosted [1]. To reduce the pressure drop associated with the use of granular adsorbents, thin film adsorbents have been employed. In the case of a PC coated with thin film adsorbents, microstructures are very often integrated to enhance their preconcentration performance [61]. It is known that this type of adsorbents has a limited adsorption capacity due to the reduced surface exposed to the analytes. Therefore, the presence of microstructures, themselves usually coated with adsorbent film, inside the microfluidic cavity greatly increases the exposed adsorptive surface, and additionally optimizes the path followed by the gas molecules, thus increasing their contact time with the adsorbent. Larger contact surface and longer residence time result in higher preconcentration performance due to the higher adsorption capacity and higher probability of the gas molecules to be trapped. Therefore, this approach enhances the sampling capacity while reducing pressure drop. Moreover, since most adsorbents have a low thermal conductivity, these structures serve also to promote a more efficient heat transfer through the adsorbent bed [16].

Different microstructures such as square [39] (Figure 5a) and cylindrical pillars [38] (Figure 5b), cross shaped micropillars [37] (Figure 5c), U- [35] (Figure 5d) and V-shaped [1] pillars (Figure 5e) can be found in micro PCs. Alfeeli and Agah [61] studied the influence of the shape and the spacing of micropillars in preconcentration performance. Crisscross shaped pillars were found to be more efficient in terms of preconcentration factor (PF) than ordered and staggered pillars. This PC contained more than 3,500 crisscross pillars with dimensions of 30 µm × 120 µm × 240 µm (see Figure 5f) and it was coated with 2,6-diphenylene oxide polymer (Tenax TA). A PF >10 000 was found for isopropanol. However, a great amount of 3D microstructures embedded within a microcavity can lead to high pressure drops.

To minimize the pressure drop, Alfeeli *et al.* [62] was the first to propose a design consisted of an array of U-shaped pillars embedded within a 7 mm × 7 mm × 0.38 mm cavity. These pillars were arranged to divide the gas flow in the forward direction and combine the resulting two flows in the reverse direction. The spacing between the reflectors (side and middle spacing) was varied to investigate its effect on the device performance. The pressure drops of different pillars arrangements were investigated at a flow rate of 1.5 mL/min. The configuration with 300 and 150 µm of middle and side spacing, respectively, exhibited a pressure drop as small as 94 Pa. In comparison configuration with 100 and 250 µm of middle and side spacing exhibited a pressure drop of 145 Pa. The same microstructure design using reflectors has been recently employed in another miniaturized PC for the quantification of n-butyl acetate, ethylbenzene and p-xylene [35] (see Figure 5b).

However, the fabrication of embedded micropillars requires high cost and even the cavities densely filled with micropillars exhibit relatively low contact surface thus reducing the sample capacity of these adsorbents. Besides, some authors observed high desorption temperatures of above 250°C for complete desorption of the analytes when using micropillars coated with thin-film adsorbents [63,64].

More recently, a new approach involving foam adsorbents instead of creating microstructures has been adopted to reduce the pressure drop and also enhance the heat transfer due to the electrical resistance of some of these foams [65].

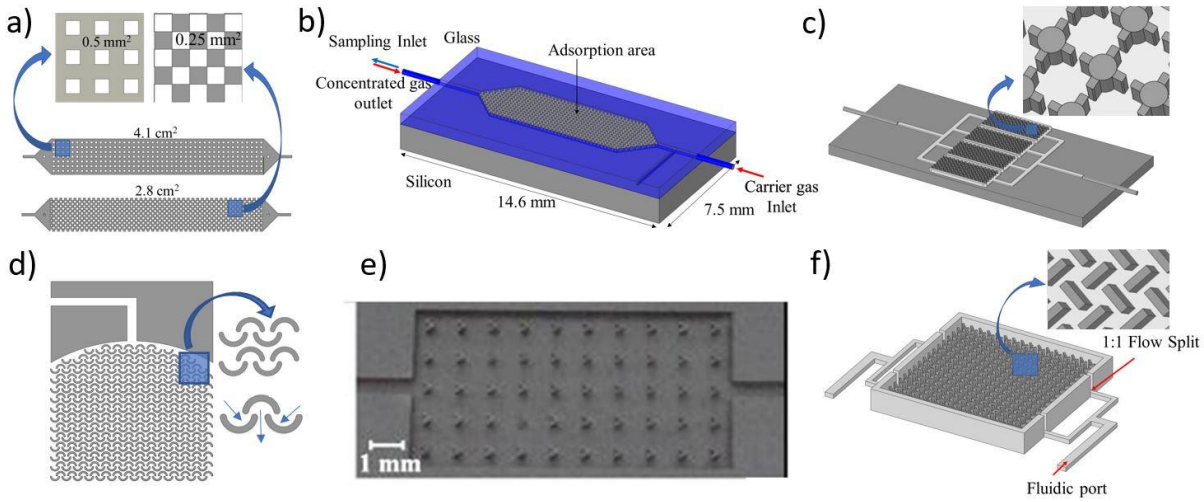

Figure 5. Preconcentrator containing a) square [39], b) cylindrical [38], c) cross [37], d) U- [35] and e) V-shaped [1] and f) crisscross shaped micropillars [61].

3.3. Preconcentrator heating technologies

During the preconcentration step, a very fast temperature ramp is needed for the flash desorption of analytes; therefore, the heating system is considered a key component in preconcentration devices. The faster this rate is, the sharper the desorption peak becomes and, thus, higher sensitivity and better chromatographic resolution can be achieved. However, since miniaturized PCs are integrated in portable instruments and most of them are battery-powered, the energy required for a flash desorption of analytes should be limited to the possible extent. Hence, a compromise between heating rate performance and energy consumption must be adopted. To this purpose, a wide variety of materials has been employed for the fabrication of these systems, as depicted in Figure 6.

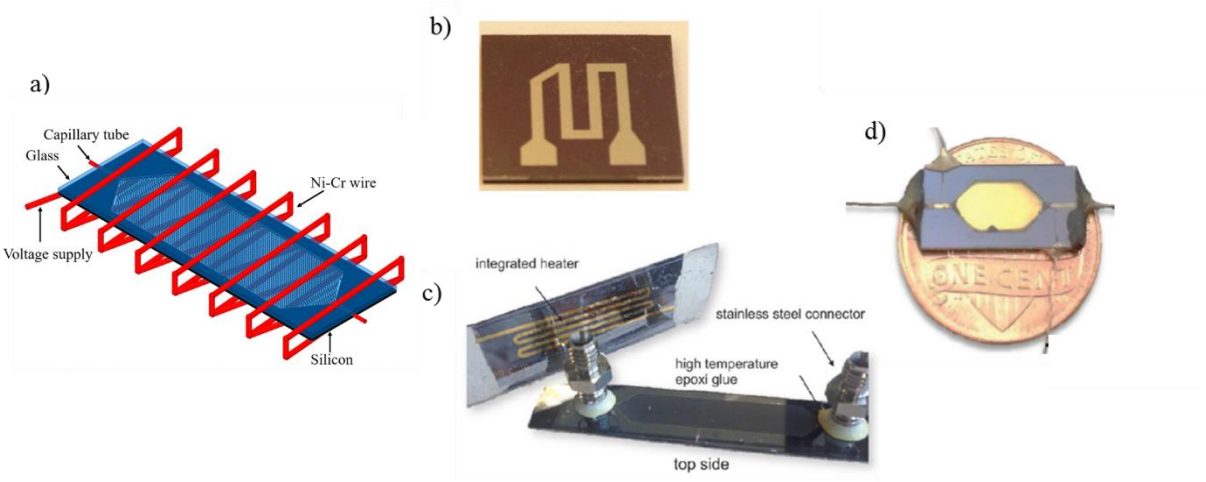

Figure 6. Diverse heating systems found in micro preconcentrators: (a) Ni-Cr wire [81], (b) platinum heater [66], (c) gold layer deposited by electron beam [39] and (d) gold layer deposited by electroless plating technology [38].

Originally, the heating system of the first generation of PCs consisted of metal wires coiled around the device [67]. Although some of these systems continue to be used today, the number of portable devices including this type of system is very small [21,66].

The material traditionally employed for these metal wires is Ni-Cr because of its extraordinary resistivity and almost constant temperature coefficient of resistance (TCR) with temperature. These features render this alloy suitable for heating and temperature measurement applications [16]. For example, Tzeng et *al*. [23] developed a micro gas chromatograph (μGC) containing a MEMS PC coiled by a 6 Ω Ni-Cr

409 wire for the detection of seven VOCs associated with lung cancer (see Figure 6a). Jian et *al*. [21]
410 employed also the same heating system for a stainless-steel tubular PC integrated in a μGC. This
411 configuration required 12 V DC to reach 320 °C in less than 4 s.

412 Nowadays, most devices are fabricated by MEMS techniques which enables the integration of heating
413 systems on the substrate. These systems consist of layers of resistive and conductive metals to form the
414 resistive heaters and the contact pads, respectively. Techniques such as e-beam evaporation [38] and
415 sputtering [27,29] are commonly used for metal deposition of a wide range of metals. Among them,
416 platinum is the most used material in micro PC's heating systems [1,5,24,27,68–70]. A resistive heater
417 made of platinum is presented in Figure 6b. Similarly to Ni-Cr, platinum has a relatively high resistivity
418 and constant TCR, being suitable to act both as a heater and a temperature sensor. Heating rates ranging
419 from 3.5 to 375 °C s^{-1} and power consumptions between 1 and 10.5 W have been reported in micro
420 preconcentrators with platinum heaters [20,26,27,33,34,36,40]. Although this metal presents better
421 adherence to substrates than other metals, an adhesive layer of titanium [24,27,33,68] or chrome [40] is
422 generally deposited beforehand to improve its adhesion to the substrate.

423 Other less common metal combinations have been employed for the fabrication of heating systems like
424 chromium-tungsten [29], chromium-nickel [12] and chromium-gold [2,39] (see Figure 6c). Despite their
425 widespread use, metal deposition processes by means of e-beam evaporation or sputtering are sometimes
426 tedious involving the use of several photomasks. To tackle this issue, Kuo et *al*. [38] proposed to use
427 electroless plating technology for the deposition of gold layers (see Figure 6d). This much simpler
428 technique is based on the chemical reduction of gold and allows the deposition of high-surface-area gold
429 layers on the surface of microchannels. Heating rates up to 75 °C s^{-1} were achieved using these resistive
430 heaters. Inkjet printing has been also employed to create resistive heaters using a gold nanoparticles-
431 based ink [32]. The main advantages of this technique are the possibility to modify the designs without
432 need for masks and the rapidity of the process.

433 Heating systems consisting of thin film resistive heaters are very convenient for MEMS-based devices;
434 however, as other microfabrication techniques, their fabrication requires to be conducted in a cleanroom.
435 Furthermore, sometimes the adhesion to the substrate is not adequate and the metal layers can detach

from the surface during the fabrication process or after several heating-cooling cycles. As an alternative to integrated thin film resistances, some groups have employed other commercially available heating technologies. Han et *al*. [28] used a micro ceramic heater located at the bottom of the substrate in their metal PC. This device was heated to 200 °C in 32 s with a power consumption of 10.14 W thus providing reasonable heating power at a very low cost. Commercial ceramic heaters have been employed in other PC [4] reaching 200 °C in 20 s but with a power supply of 61 W. Other commercial solutions such as heating cartridges have been used in PCs with relatively high thermal mass [10]. Homemade flexible membranes have been fabricated by sandwiching a thin Ni-Cr wire with two Kapton tapes [16]. This membrane was wrapped around a cylindrical PC. By applying 14.6 W of power, the PC reached 315°C in 12 s.

Apart from the heating rate, power consumption is a vital aspect of any component of a portable instrument as it can be critical for the autonomy of the whole system. Unfortunately, these data are not systematically provided for all the preconcentrators in the published literature (see Tables 1-4) thus making difficult to evaluate the impact of their integration in a real portable instrument. Therefore, it is recommended to provide power consumption in future publications in the field to facilitate this evaluation.

3.4. Fluidic connections

Fluidic interfacing between miniaturized components is a critical aspect in µGC. The issues associated with these components such as losses by adsorption, dead volumes or leaks may condition the performance of the GC system. In the particular case of PCs, the fluidic connections limit their maximum operation temperature thereby reducing the efficiency of the analytes' desorption. Ideally, connectors must be reliable and low-cost, have a low dead volume and they should allow the interfacing in a reversible manner. However, most of the fluidic connections used in miniaturized PCs exhibit only some of these features.

The most common method is the use of adhesives to glue fused silica capillaries to the miniaturized PCs [34,53]. Deactivated fused silica is the preferred material used for capillaries due to their inertness, cost and variety of diameters, although the use of nickel capillaries have been also reported [27]. Usually, thermal resistant epoxy or glue are applied around the capillaries and these are inserted into the inlet/outlet ports. Then, more epoxy is applied around the connection to assure hermetic sealing. These adhesives can be cured at room temperature but the curing process may also be conducted at higher temperature to speed up the process. Some examples of high temperature adhesives employed are Duraseal 1531 [53] and Duralco 4703 [34]. In some PCs, additional ports are used to introduce the adsorbent into the PC [53]. Other epoxy resins such as Duraseal [6] or Stycast 2850FT [24] are applied to hermetically seal these ports once the adsorbent introduced.

In other devices, epoxy was employed to fix Nanoport assemblies [8,34,36]. Capillaries and flexible tubing can be easily connected to these ports by using commercial fittings. Swagelok® stainless steel connections have been also glued using Loctite Hysol 9492 on the glass die of a micro PC [39]. In the ceramic PC developed by Zaidi et *al*. [22], two hoses of 3.5 mm of outer diameter were glued to the main structure of the device in which flexible tubes were inserted.

Some research groups use additional metal parts to accommodate commercial gas flow connectors. The use of these connectors diminishes the risk of leakage and allows the replacement of a single component of the µGC system. Janssen et *al*. [30] built a housing made of two different aluminum parts using drilling and Computer Numerical Control (CNC) technology. Standard compression fittings were integrated in these parts to connect the inlet and outlet of the PC. In 3D the printed PC proposed by Huang et *al*. [16], a standard port thread was machined enabling the use of commercial gas fittings. They used PEEK (polyetheretherketone)-based fittings from IDEX Health Science to connect flexible tubing to the port ensuring leak-free connections under a pressure up to 1 MPa (10 bars) and temperature up to 343 °C. Rodríguez-Cuevas et *al*. [4] fabricated PEEK reducing unions equivalent to the standard stainless steel unions provided by Swagelok. These unions were connected at both sides of the PC facilitating its integration into the GC system and thermally insulating the PC.

Qin and Gianchandani [24] used standard compression fittings between the two modules of their micro GC whereas the different components were connected using micromachined gas flow connectors. The small size of these latter allowed to arrange the components in a compact manner.

Other heat resistant materials such as polymide have been used for fluidic interfacing: Han et *al*. [28] connected deactivated fused silica capillary tubes using customized polyimide adapters which can operate for 2 h at 300°C.

3.5. Adsorbents

A great part of the PC performance relies on the adsorbent material employed. Its textural properties and chemical affinity towards analytes will be determinant for the efficiency of the adsorption and desorption processes. In this regard, the desired features for an adsorbent are:

- Selectivity towards the target compounds. Ideally, the adsorbent should capture only the analytes of interest. In practice, the adsorption of a single compound is usually very challenging. However, during the preconcentration, some interfering species can be eliminated by placing some trapping devices in the upstream sampling flow.
- High specific surface area. A large number of adsorption sites generally increases adsorption capacity and prevents early breakthrough of the analytes.
- Moderate strength interactions with the adsorbate, enabling considerable adsorption capacity at room temperature and desorption at reasonable higher temperatures.
- Thermal stability. Adsorbents are subjected to temperature cycles and their performances must last throughout time.
- Low pressure drops and good thermal conductivity to minimize energy consumption and promote an efficient thermal desorption of analytes.

Traditionally, adsorbents have been distinguished in two categories: granular and thin films. Nonetheless a new category, foam adsorbents, has been in constant development over the last years. These three groups are displayed in Figure 7.

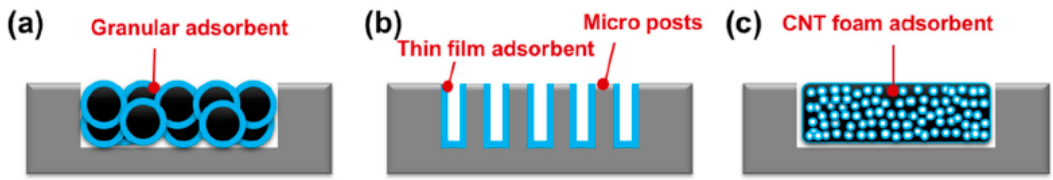

Figure 7. Schematics of several types of adsorbents: (a) granular, (b) thin film and (c) foam adsorbents [36].

Granular adsorbents have generally higher adsorption capacity than other types of adsorbents as the grains are compactly packed, thus occupying almost all the volume available inside the PC. However, the complete filling of the microfluidic cavity usually results in high pressure drops. On the contrary, thin-film adsorbents exhibit very low pressure drop [62] as only the surface of the PC is covered with the adsorbent. However, due to the small amount of the material deposited, their adsorption capacity is limited. On the other hand, the new generation of foam adsorbents tend to reduce the pressure drop while keeping a relatively high adsorption capacity [34,36]. Furthermore, some of these foams have high thermal conductivity leading to an improvement in the heat transfer from the adsorbent to the adsorbates facilitating the desorption and decreasing the power consumption of the device [65].

3.5.1. Granular adsorbents

Granular adsorbents are usually introduced inside the PC by suction [29,32,38,56]. Most of granular adsorbents are carbon-based. Among them, graphitized carbon blacks are traditionally used for VOC preconcentration due to their hydrophobic character, which make them ideal candidates for VOC sampling in humid environments. The most commonly used are Carbopack® B, which is recommended for the capture of C5-C12 molecules such as isoprene [28], and Carbopack® X, which is more suitable to trap C3-C9. Because these adsorbents are appropriate to trap compounds of intermediate volatility, they are considered to have medium strength. Most commonly, a combination of these adsorbents is employed to enlarge the range of analytes trapped [5,6,24]. Qin and Gianchandani [24] use a combination of Carbopack-X and Carbopack-B, to preconcentrate a mixture of 19 VOC including aromatics, alkanes and halogenated compounds. Lee et *al*. [15] preconcentrate a gas mixture containing 50 VOC that was subsequently separated and detected by four independent GC columns and PID detectors. Other type of carbon-based granular adsorbents are the molecular sieves such as the ones of the Carbosieve and Carboxen series. These materials contain micropores in which very volatile compounds (C2-C5) can be trapped. Carbosieve II has been used for the preconcentration of ethylene [22,30]. Rydosz et *al*. [7] used Carboxen 1012 for the preconcentration of acetone. A combination of molecular sieve with graphitized carbon blacks is usually employed for the preconcentration of molecules of low and intermediate volatility. Jian et *al*. [21] developed a preconcentrator containing 3

mg of Carbopack® B, 2 mg of Carbopack® X, and 1 mg of Carboxen® 1000 for the analysis of 10 VOC mixture. In these cases, particular attention should be paid to the location of the adsorbents and the flow direction. Analytes of medium volatility are strongly adsorbed in molecular sieves, thus rendering difficult the subsequent desorption. Therefore, for sampling, adsorbents should be placed from the weaker to the stronger while the desorption should be carried out in the opposite direction.

The surface of carbon-based adsorbents is generally relatively non-polar preventing the adsorption not only of water, but also other polar VOC. To enhance their adsorption capacity and selectivity towards polar VOC, Wang et *al*. [71] coated commercial graphitized carbons (Carbopack B and Carbopack X) with room-temperature-ionic-liquids (RTIL). The RTIL-coated adsorbents exhibited ~2.5 times larger 10% breakthrough volume (V_{b10}) for organophosphorus vapors than the untreated adsorbents. Furthermore, V_{b10} values of the four non-polar reference vapors tested were 11–26 times smaller for the RTIL-coated than for the untreated counterpart.

Porous polymers as HayeSep® [72] and Tenax® [27,29] are also commonly employed in preconcentration devices. Chappuis et *al*. [27] employed this latter polymer for the preconcentration of volatile tobacco markers. McCartney et *al*. [29] reported the preconcentration of a wide variety of VOC with a low-cost PC filled with Tenax. Using this device, Limit Of Detection (LOD) down to 22 ppb were achieved with only 2 min of sampling, the sampling volume being not provided by the authors.

Metal organic frameworks (MOF) have been used as preconcentration materials for VOC due to their large specific surface and variety of chemical properties. HKUST-1 ($Cu_3(BTC)_2$) is a microporous MOF with a very high specific surface area (1100-1700 $m^2\ g^{-1}$) formed by copper nodes with 1,3,5-benzenetricarboxylic acid linkers between them [73,74]. This material is commercially available as Basolite™ C300 and has been used for the preconcentration of aromatic compounds [10,31]. Another well-established MOF, UIO-66 ($Zr_6O_4(OH)_4(BDC)_6$, BDC=1,4-benzenedicarboxylate), having also high surface area (over 1000 $m^2\ g^{-1}$) has been used for the capture and preconcentration of acetone [73,75].

A general issue in gas preconcentration is the lack of selectivity of the employed adsorbents, which leads to the preconcentration of analytes but also of interfering species. To tackle this issue, Zampolli et *al*. [13] synthetized in 2009 a quinoxaline-based adsorbent named QxCav (see Figure 8a) for the selective preconcentration of aromatic compounds. This adsorbent has cavities of 8.3Å in which BTEX are adsorbed by means of weak CH–π interactions with the walls, whereas other non-aromatics molecules such as aliphatic compounds and water vapour are not retained. The same group recently developed an improved version of the adsorbent called EtQxBox [20]. Its structure is displayed in Figure 8b. In this complex, aromatic VOC are selectively adsorbed, and toluene, ethylbenzene and xylene (TEX) are adsorbed more strongly than benzene. The difference in the strength of interactions renders possible the benzene desorption at lower temperatures compared to TEX. This singularity allows the separation of analytes during the preconcentration step itself by controlling the desorption temperature and thus a shorter GC column can be used for separation reducing the analysis time.

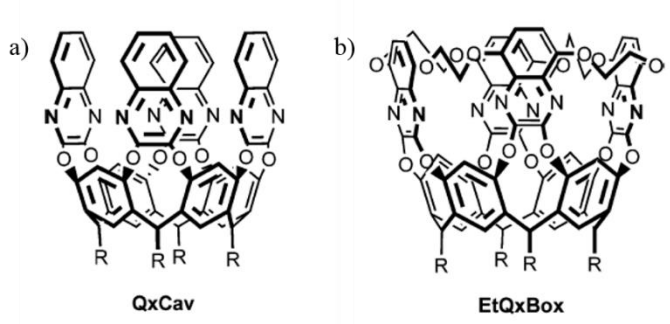

Figure 8. QxCav (a) and EtQxBox (b) cavitands employed for the selective preconcentration of aromatic compounds [20].

3.5.2. Thin film adsorbents

This type of adsorbents is generally introduced into the microfluidic cavity in a liquid dispersion at a specific concentration. The dispersion is inserted in the microfluidic cavity by depression and the solvent is then evaporated at room temperature, leaving a film on the inner surface of the cavity [1,38,40]. Gregis et *al*. [8] employed a dispersion of a commercially available dealuminated zeolite (DaY) in ethanol to deposit a uniform 13 µm thick film. This system allowed the detection of toluene, o-xylene, propanol and cyclohexane at the low ppb levels, except for the cyclohexane. Other types of materials such as

591 single-walled carbon nanotubes (SWCNT) have been deposited inside a micro PC for the quantification
592 of VOC at trace levels [37,40]. The use of this adsorbent is advantageous due to the large aspect ratio,
593 high effective surface area, chemical and thermal stability, and hydrophobicity. Other films have been
594 synthetized inside the preconcentration device itself. For example, Tzeng et *al*. [23] and Wong et *al*.
595 [76] presented in-situ-synthesized carbon adsorbent films for VOCs analysis. To this purpose, cellulose
596 was inserted in a microfluidic cavity and then pyrolyzed at 600 °C under a nitrogen atmosphere to form
597 the porous carbon film. The resulting adsorbent (2 mg) had a specific surface area of 308 $m^2 g^{-1}$ and the
598 whole system exhibited a huge preconcentration factor of 13,637 for toluene (calculated as the ratio
599 between the peak area obtained with and without the preconcentrator). Almazán et *al*. [39] synthetized
600 silicalite-1 inside of a micro PC with diverse microstructures. These microstructures increased the inner
601 surface of the PC and thus the amount of zeolite deposited compared to the empty PC. All PCs filled
602 with zeolite thin films showed higher preconcentration efficiency than their fixed bed counterpart, due
603 to the uniform zeolite distribution along the inner surface. This homogeneity improved the gas–solid
604 contact and thus adsorption. Furthermore, by introducing pillars in the cavity, the amount of absorbent
605 coated increases, thereby, the adsorption capacity increases. A uniform deposition of the adsorbent is
606 also important for a more homogeneous heating transfer during the desorption because the adsorbent
607 film is directly deposited on the thermal conductor. Therefore, full desorption is more likely to occur,
608 and it will be conducted simultaneously to the same extent across the adsorbent bed. To increase the
609 inner PC surface, Zhao et *al*. [35] proposed the formation of silicon nanowires as a surface template
610 prior to the deposition of Tenax® inside the cavity. The use of this template increased the
611 preconcentration performance of more than 188 % for n-butyl acetate compared to the PC only filled
612 with Tenax®.

613

614 ### 3.5.3. Foam adsorbents

615 To enhance the adsorption capacity of the preconcentration devices without greatly increasing the
616 pressure drop, foam adsorbents have been recently developed. Lee and Lim [36] employed a carbon
617 nanotube (CNT) foam for the preconcentration of gaseous ethane. For comparison purposes, the same

PC was filled with Carbosieve™ SIII, a granular absorbent with a surface area of 1000 m^2/g and mean pore diameter of 1 nm. Pressure drop was measured in both devices for flow rates from 1 to 5 mL min^{-1}. Pressure drops using the molecular sieve varied from 2061 to 9919 Pa whereas it was more limited with the CNT foam, where pressure drops ranged between 445 to 2078 Pa. Therefore, the use of this adsorbent decreased five times the pressure drops inside the PC.

Jang et *al*. [65] synthetized a carbon nanotube (CNT) sponge for the preconcentration of aromatic VOC. 5 mg of the CNT sponge were packed in a ¼" Pyrex glass tube (4 mm i.d. and 40 mm length). The tube was connected using stainless steel fittings in which two porous metal frits were inserted to ensure electrical contact with the CNT sponge. Due to its electrical resistance (15-20 Ω), this material can be rapidly heated at a rate of 400 °C/s by simply applying a voltage of 26 V. This feature leads to an efficient heat transfer from the adsorbent to the adsorbates promoting a quantitative desorption (>96%) with low power consumption. Using 100 mL sample at concentrations of 36–63 ppb (v/v), preconcentration factors (calculated as the ratio of the peak intensities obtained with the preconcentrator and the sampling loop) of 88 (benzene) and 323 (toluene and o-xylene) were observed.

Lee et *al*. [34] developed a micropreconcentrator using a metal organic framework embedded in a metal foam (MOFM) as an adsorbent. To evaluate its performance, commercial adsorbents (RAD145 and Carbopack B) were packed in the same micropreconcentrator. The MOFM micropreconcentrator exhibited pressure drops 4-3 times lower than the one packed with commercial adsorbents. Furthermore, the analysis of a BTEX mixture revealed that the preconcentration factors achieved with MOFM PCs were 2.6 and 4 times higher than the one packed with commercial adsorbents at a desorption temperature of 150°C.

3.6. Evaluation of preconcentration performance

The existence of many factors affecting the performance of gas preconcentrators renders difficult to establish the basis for a proper and easy comparison between different devices. Traditionally, the performance of gas preconcentrators has been characterized by a figure of merit called preconcentration factor (PF). Nevertheless, there is no general consensus among the authors and different definitions have

been adopted for the PF. In several studies, the PF is defined as the ratio between the maximum concentration measured at the desorption step and the initial concentration of the injected sample [34,77,78]. In some others, PF is calculated as the ratio between either the peak areas [1,29,38] or the peak heights [1] obtained with the PC without the adsorbent and the PC packed with the adsorbent. Other authors determine PF as the ratio between the peak area obtained using the GC system with and without PC [36], which is close to the very first definition above. However, although PF is frequently used to characterize the PC performance, it is not an intrinsic property of the preconcentrator itself [64] as it depends on several external factors including concentration of the analyte, sampling flow rate and dead volumes in the GC system. Among the intrinsic properties of the PC, the ability to obtain a flash desorption of analytes thus producing sharp chromatographic peaks is of great importance. Figure 9 represents the preconcentration factor as a function of the heating rate (°C/s) used for the desorption of different VOC. These data have been extracted from the data reported in Table 3 and Table 4 when both parameters were given in the corresponding papers [28,32–34,36,38]. This figure seems to show that the preconcentrator factor increases significantly with the heating rate for a heating rate value higher than 40°C/s although no significant influence of this parameter was highlighted between 5 and 40°C/s. This behaviour seems to be independent of the nature of the adsorbent. Unfortunately, there is little data on the Figure 9 which implies that these interpretations should be taken with caution. For future publications in the field, we recommend that the authors provide both data on the preconcentration factor and the rate of desorption temperature increase. Thereby, whatever the definition of PF considered, this parameter can be very useful when comparing the performances of similar devices under the same experimental conditions, but it should be used with prudence when comparing various preconcentration devices at different experimental conditions. The use of this parameter is not ideal, however, the preconcentration factor is the only parameter provided in most of the publications to evaluate the performance of the preconcentration step.

Indeed, the PF results are in general terms linear dependent with the sample volume, unless they are close to the saturation of the adsorbent. Therefore, PF of a single device may vary several orders of magnitude only by increasing the sample volume as illustrated in Figure 10 for the series of experiments performed with granular adsorbents shown on the right part of this figure [1,7,30,32,33]. For example, in the literature, some authors have achieved PF values as high as 800000 whereas some others were as lower as 5.

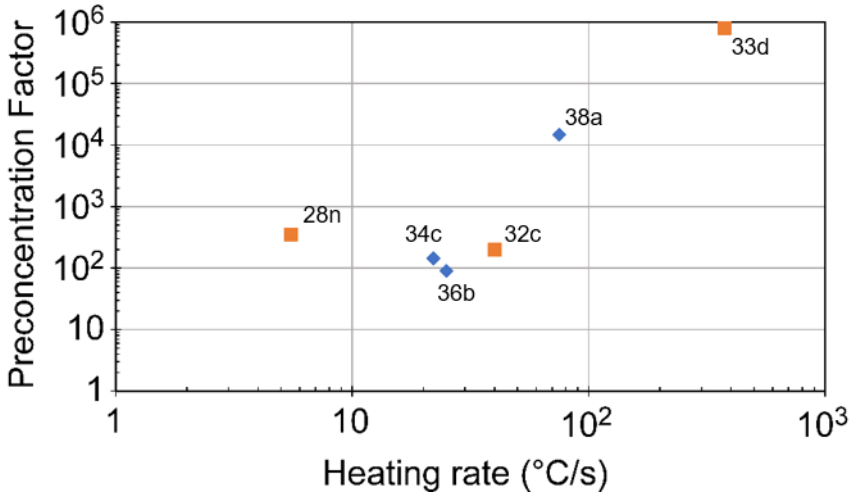

Figure 9. Preconcentration factor (as defined by the authors) of different preconcentrators as a function of heating rate: preconcentrators packed with commercial granular adsorbents (■) [28,32,33] and preconcentrators packed with other type of adsorbents (◆) [34,36,38]. The subscripts indicate the different methods employed for the calculation of the preconcentration factor: "a" ratio of the concentration peak area of the PC packed with adsorbent to that of the PC without adsorbent, "b" ratio between peak area of the detector with and without the presence of a PC, "c" ratio between the maximum concentration measured at the desorption step and the initial concentration of the injected sample gas, "d" ratio of the volume of the air sample collected to the volume in which that same mass is contained at the point of detection, "n" not mentioned.

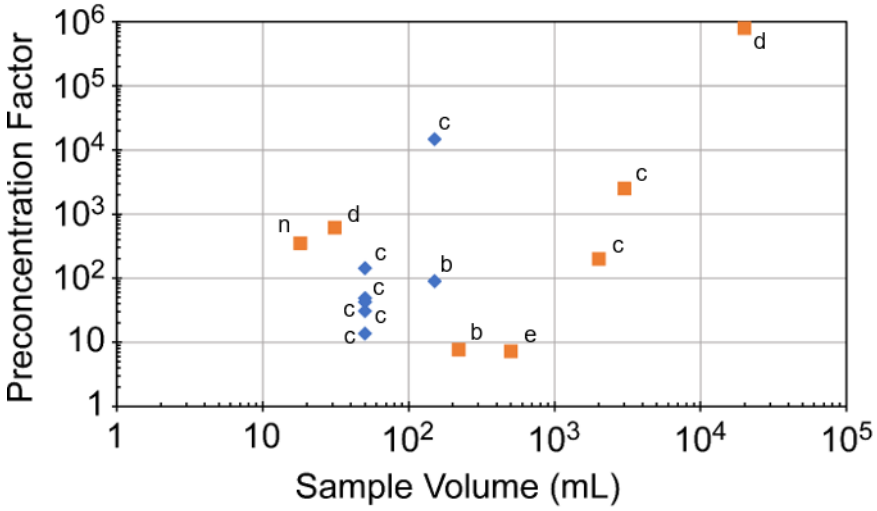

Figure 10. Preconcentration factor of different preconcentrators as a function of sample volume: preconcentrators packed with commercial granular adsorbents (■)[1,5,7,28,30,32,33] and preconcentrators packed with other type of adsorbents (◆) [34,36,38,39]. The subscripts indicate the method employed The subscripts indicate the different methods employed for the calculation of the preconcentration factor: "a" ratio of the concentration peak area of the PC packed with adsorbent to that of the PC without adsorbent, "b" ratio between peak area of the detector with and without the presence of a PC, "c" ratio between the maximum concentration measured at the desorption step and the initial concentration of the injected sample gas, "d" ratio of the volume of the air sample collected to the volume in which that same mass is contained at the point of detection, "n" not mentioned.

In light of these discrepancies, it would be more convenient to use a different parameter to evaluate the preconcentration performance of a gas preconcentration device which takes into account the sample volume. We propose to use a new figure of merit called Normalized Preconcentration Efficacy (NPE) presented in equation 1. This parameter represents the efficacy of the preconcentration step compared to an ideal scenario, an injection using sampling loop where all the analyte molecules collected are injected into the column. Therefore, NPE will range between 0 and 100%. To calculate this parameter, we recommend using of a sampling loop with a known volume (i.e., 20-200 µL), a commercial capillary column appropriate for the separation of the target compounds and a benchtop GC equipped with an FID. If the use of a sampling loop is not possible, the injection of a known volume of gas can be conducted manually using a gas-tight syringe.

To determine NPE, a gas sample with a specific concentration will be first analysed using the sampling loop connected to the benchtop GC-FID. Then, the sampling loop will be replaced by the gas preconcentrator and a gas sample with the same concentration will be analysed again. Obviously, the

sample volume used in both tests will be different and must be considered. Therefore, the preconcentration efficacy will be calculated as the ratio between the peak areas normalized by the injected volume in each test as shown in equation 1,

$$NPE\ (\%) = \frac{A_{PC}/V_{PC}}{A_{SL}/V_{SL}} \cdot 100 = \frac{A_{PC} \cdot V_{SL}}{A_{SL} \cdot V_{PC}} \cdot 100 \qquad \text{Eq. 1}$$

where A_{PC} is the peak area measured by the GC-FID when using the preconcentrator, V_{PC} is the volume of the air sample collected on the preconcentrator, A_{SL} is the peak area measured by the GC-FID when using a sampling loop, and V_{SL} is the volume of the sampling loop. Note that peak areas must be measured using the same benchtop equipment at the same experimental conditions. Alternatively, the corresponding peak intensities can replace the peak areas considered in equation 1.

The sampling loop represents the ideal conditions in which all the analyte molecules collected are injected into the column, thus, it can be considered as a reference. As the measurements using the sampling loop and the gas preconcentrator are conducted at the same experimental conditions (length and type of chromatography column, temperature program, detector), the variations between the two peak areas can be only attributed to the features of the gas preconcentrator. Therefore, unlike the preconcentration factor, this parameter can be used to compare the performances of different gas preconcentration devices. Furthermore, NPE considers the ratio between the sample volumes, and thus, it is independent of the gaseous sample volume used for its determination.

Sometimes, the preconcentration performance is evaluated using the whole GC system instead of the single PC device. In this case, the sensitivity improvement due to the integration of a preconcentration cannot be assessed and the system is evaluated as a whole. Considering the GC system, it is very common to use the limit of detection (LOD) in concentration units like parts per million (ppm) or parts per billion (pbb) to describe the sensitivity of the instrument. Chromatographic peaks areas increase linearly when the sample volume increases [4,10]. For instance, a relatively small sample volume will

provide better temporal resolution while a large volume will provide a lower LOD. Therefore, since LOD strongly depends on the sample volume, it is more accurate to the describe the sensitivity of each system in a non-volume dependent magnitude such as the lowest detectable mass of analyte. This mass can be calculated as the lowest LOD achieved multiplied by the sample volume. Only few publications provide sensitivity in mass units, but this parameter has been calculated for several portable GC instruments and presented in Table 1 and Table 2 for comparison. Using this parameter, variation of several orders of magnitude can be observed among different portable GC systems (see Table 1 and Table 2) whereas LOD of these instruments are very similar when they are expressed in ppm or ppb. For instance, the GC developed by Alberto et *al.* [4] present an LOD of 0.06 for benzene whereas the GC reported by Jiang et *al.* [21] exhibits an LOD of 0.02 ppb for this chemical; however, this latter has a sensitivity of 90 pg while the sensitivity of the first one is only 3.6 pg.

3.7. Applications

In the last decades, the quantification of a wide variety of VOC molecules has generated considerable research interest. These molecules are very often found at trace levels; therefore, portable GC integrating PC units have been developed for a broad spectrum of applications. Since there is increasing evidence of the effects of air quality on human health [80,81], the majority of the portable analytical systems developed by research groups are focused on air quality and occupational exposure monitoring.

Figure 11 represents the sensitivity (in pg) of different portable GC as a function of air sample volume (mL) used for VOC detection with either photoionization detector (PID) [4,10,11,15,17–21] or other detectors such as thermal conductivity detector (TCD) [12], chemiresistor (CR) [2,6], capacitive detector (CD) [24] and metal oxide sensors [8,13,23,25]. The data presented in Figure 11 have been extracted from the literature when both sensitivity (in pg) and gas sample volume were available. These data are detailed in Table 1 and Table 2. Regarding the own definition of the sensitivity (in pg) already mentioned in this manuscript, the sensitivity should be independent of the sample volume. This is moreover more or less the case for the portable GC coupled to other detectors different from PID with preconcentrators packed with commercial granular adsorbents [2,6,22,24] and other adsorbents [8,12,13] since most of them exhibited sensitivity around 500-2400 pg, except two of them where sensitivity values were 22611

pg [8] and 5736 pg [22] whatever the nature of the adsorbent used. This obvious trend is not observed for the GC coupled to PID [4,10,17,18,20,21] but this observation could be explained by the variation of other key parameters in these studies such as the heating rate.

In Figure 11, the general trend shows that, among the portable GC integrating miniaturized preconcentrators, GC-PID are usually much more sensitive than the portable GC coupled to other detectors. However, if we do not consider Plasma or discharge micro PID (D-µPID) [82,83], photoionization detectors are more specific to unsaturated organic compounds such as aromatic species and carbonyl compounds and they are not able to quantify other VOC with higher ionization energies, whereas other detectors such as capacitive detectors or metal oxide sensors are more universal and are able to detect a large number of VOC families.

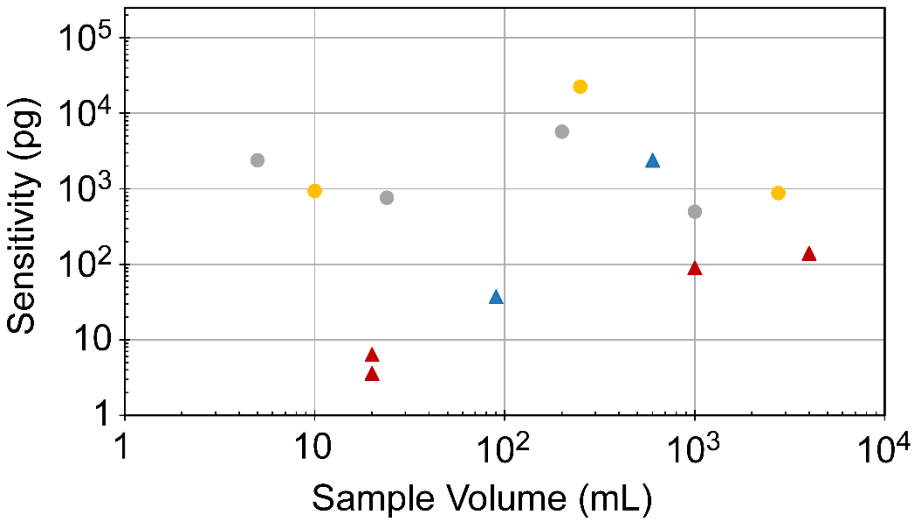

Figure 11. Sensitivity of different portable GC as a function of sample volume: portable GC-PID with preconcentrators packed with commercial granular adsorbents (▲) [4,10,18,21] and other adsorbents (▲) [17,20] and portable GC coupled to detectors different from PID with preconcentrators packed with commercial granular adsorbents (●) [2,6,22,24] and other adsorbents (●) [8,12,13].

Qin and Gianchadani [24] developed a micro gas chromatography system in which all the components were microfabricated (see Figure 12a). This device was able to detect a mixture of common indoor air pollutants including alkanes, aromatic hydrocarbons, aldehydes, halogenated hydrocarbons and terpenes at ppb levels. Wang et *al*. [6] developed a belt-mountable µGC prototype to monitor personal exposure

able to analyse a sample containing a mixture of 21 VOC in 3.5 min (see Figure 12b). The PC consist of two microfluidic cavities separated by rows of pillars and packed with ~2 mg of Carbopack B and Carbopack X. This system has a LOD from 16 to 600 ppb depending on the compound. Trzciński et *al*. [20] reported the fabrication of a sensor prototype for environmental benzene monitoring. This device was packed with a customized adsorbent that selectively trap benzene over the rest of aromatic compounds. Garg et *al*. [12] developed a µGC for the detection of hazardous air pollutants such as benzene, toluene, tetrachloroethylene, chlorobenzene, ethylbenzene, and p-xylene (see Figure 12c). The instrument integrates a MEMS-based PC with embedded pillars coated with a thin layer of Tenax TA as adsorbent. By sampling for 10 min at a flow rate of 1 mL/min, a limit of detection of ~1 ng was achieved.

More recently, portable analytical systems for the detection of explosives have been also reported. Since these compounds easily degrade into a variety of species, the analysis is often focused on these by-products instead on the explosive molecule itself. Mohsen et *al*. [1] designed a µGC for the detection of an explosive-related compound, namely ortho-nitrotoluene. The system consisted of a silicon PC and a GC column coupled to a chemical gas sensor and allowed to detect down to 365 ppb of this compound in the presence of interfering compounds such as toluene and water. Collin et *al*. [2] presented a very compact GC for the quantification of 2,4,6-trinitrotoluene (TNT) derived products (see Figure 12d). The miniaturized PC consisted of a cavity etched in a silicon substrate, sealed with a Pyrex plate and packed with 2.4 mg of Carbopack B. For 1 L sample, LOD of 0.30 ppb (2161 pg), 0.067 ppb (499 pg), and 0.12 ppb (894 pg) were achieved for 2,3-dimethyl-2,3-dinitrobutane (DMNB), 2,6-dinitrotoluene (2,6-DNT) and 2,4-dinitrotoluene (2,4-DNT), respectively.

Ethylene monitoring is of great interest to predict shelf life of climacteric fruits such as bananas. In this context, Zaidi et *al*. [22] presented a portable GC system with an integrated miniaturized PC packed with Carbosieve SII for the selective detection of ethylene (see Figure 12e). For a sample volume of 200 mL, the instrument has a LOD of 25 ppb (5,736 pg) and no interference was observed from other ripening gases such as CO_2, O_2 and humidity.

The low LOD and continuous monitoring of ethylene allow to identify any issues with the goods thus avoiding unnecessary transports and reducing costs and pollution emissions.

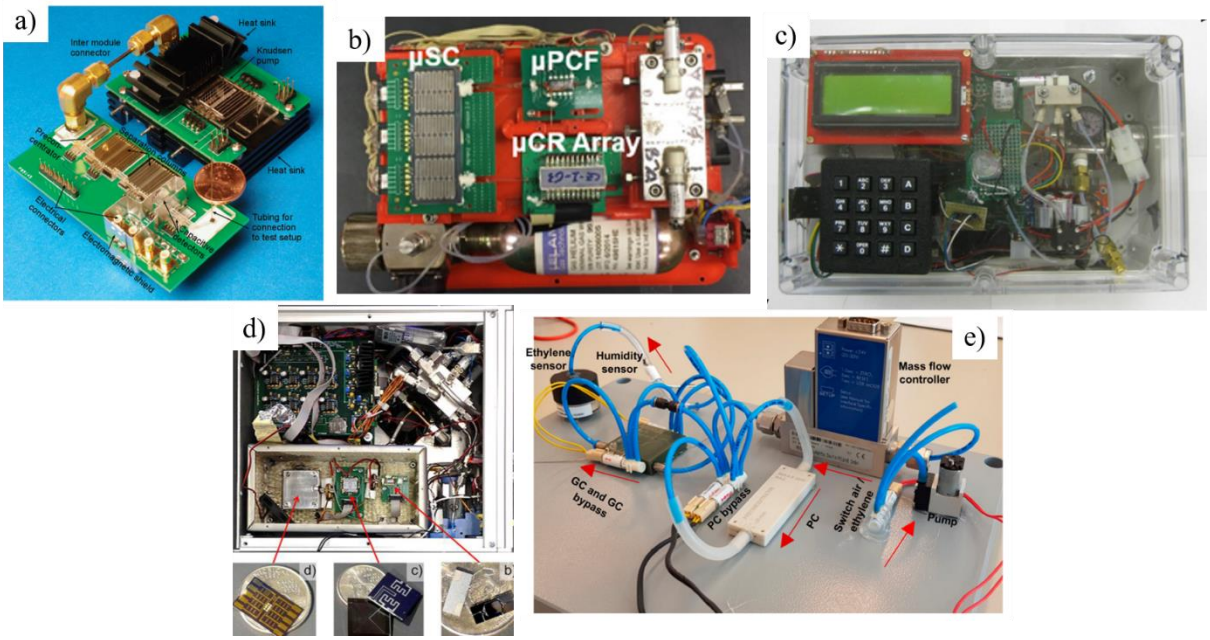

Figure 12. Pictures of portable chromatographs from a) Qin and Gianchadani [24], b) Wang et *al.* [6], c) Garg et *al.* [12] d) Collin et *al.* [2] and e) Zaidi et *al.* [22].

Recent progress in medicine showed that some VOC such as acetone, ethanol, isoprene or heptane are biomarkers of certain diseases including asthma, chronic obstructive pulmonary disease and lung cancer [84,85]. These biomarkers are present in human breath at the ppb level; therefore, an accurate and sensitive analysis in near real time may constitute a non-invasive method for early diagnosis of these serious diseases. To this purpose, several μGC integrating PC units have been developed. Gregis et *al.* [8] reported a μGC to monitor four biomarkers (propanol, toluene, o-xylene and cyclohexane) associated to lung cancer. The PC was composed of a microcavity with embedded micropillars filled with zeolite DaY. This system exhibited LOD of 24 ppb (22,611 pg), 5 ppb (5,428 pg), 21 ppb (12,904 pg) and 112 ppb (96,379 pg) for toluene, o-xylene, propanol and cyclohexane, respectively for a sample volume of 250 mL. The LOD obtained for the first three compounds was maintained even in samples containing CO_2 and water levels similar to those found in real human breath samples. Han et *al.* [28] reported a low-cost PC for the preconcentration of isoprene, a typical biomarker of chronic liver disease. This device was made of copper and packed with 20 mg of Carbopack X. Isoprene concentrations as low as

10 ppb (501 pg) can be achieved for a 18 mL sample when this PC is coupled to a GC-FID. However, despite the great advances made in the last years, high concentration of CO_2 (~ 40,000 ppm) and the relative humidity of 100 % at 25 °C [8] present in human breath make accurate analysis of human breath still a challenge.

4. Conclusions

Recent trends in the development of miniaturized gas preconcentrators for portable gas chromatography are reported in this paper. Alternative fabrication techniques able to build miniaturized devices, different fluidic layouts promoting flow uniformity, new adsorbent materials with low pressure drops and the integration of standard gas flow fittings for more reliable interfacing are some of the advances made in the last years. These developments can improve the overall features of portable GC like energy consumption, cost, sensitivity and reproducibility.

Nowadays, MEMS-based techniques such as photolithography and dry etching continue to be the most popular for the fabrication of micro PC. Even though these techniques are the most convenient technology for micro fabrication of preconcentrators, they are not free of drawbacks. The fragility of the devices produced by this technology and the lack of standards fluidic interfacing are major challenges as it is evidenced by the presence of few MEMS-based PCs in commercial instruments. Furthermore, despite their potential for high-volume production, the development of these devices involves the use of cleanrooms facilities what can be expensive and time-consuming for scientific research.

Given this reality, some new approaches are being adopted. Laser etching, micro-milling or additive 3D printing in metal are three big promises to overcome the problems in the preconcentrators derived from the MEMS technology. The opportunity of using alternative materials other than silicon opens a new range of possibilities regarding PC design and integration of standard fluidic connections. Nonetheless, a balance must be pursued since these other techniques do not achieve the performance of MEMS-based PC in terms of power consumption, heating rates and consequently narrowness of chromatographic peaks.

Traditionally, granular adsorbents have been used in miniaturized PC. Due to the issues associated with high pressure drops and poor heat transfer, thin film adsorbents were lately developed. Currently, a third generation of promising adsorbents, foam-based adsorbents, is being developed. This new type of materials provides a balance between a reasonable adsorption capacity and limited pressure drop. Moreover, foams exhibited better heat transfer efficiency than their granular and thin film counterparts due to its electrical resistance, resulting in a quantitative desorption with lower power consumption. However, commercial granular adsorbents are still frequently used in many devices since their behaviour and characteristics are well-known.

Finally, there is a need to establish a standard metric to evaluate the preconcentration performances of the different PCs that allows to compare the results provided by the different authors. In this review, we propose the use of the Normalized Preconcentration Efficacy (NPE) in future publications as a figure of merit to overcome this problem.

In addition, in order to evaluate the overall analytical GC performances, LOD should be expressed in both ppb or ppm levels but also in pg or ng to introduce the sample volume considered in the experiments. Indeed, the LOD and PF are linear dependent with the sample volume as long as we are far below the saturation of the adsorbent. This sample volume, the heating rate and the power consumption should be also mentioned in all future publications in the field. This set of information will facilitate the comparison of analytical performances between PCs reported in several studies and LOD between µGC.

Acknowledgments

This publication is part of a project that has received funding from the European Union's Horizon 2020 research and innovation program under the Marie Skłodowska-Curie grant agreement No 643095, the Clean Sky 2 Joint Undertaking under the European Union's Horizon 2020 research and innovation program under grant agreement No 687014 and the LIFE program, grant number LIFE17 ENV/FR/000330. This project was also supported through the European project ELCOD. The ELCOD project was implemented as a part of the INTERREG V Oberrhein/Rhin Superieur program and was

supported by the European Regional Development Fund (ERDF) and the co-financed project partners Region Grand Est in France and the countries of Baden-Württemberg and Rhineland-Palatinate.

The authors are also grateful to the CNRS, the University of Strasbourg and In'Air Solutions.

References

[1] Y. Mohsen, H. Lahlou, J.-B. Sanchez, F. Berger, I. Bezverkhyy, G. Weber, J.-P. Bellat, Development of a micro-analytical prototype for selective trace detection of orthonitrotoluene, Microchemical Journal. 114 (2014) 48–52. https://doi.org/10.1016/j.microc.2013.12.001.

[2] W.R. Collin, G. Serrano, L.K. Wright, H. Chang, N. Nuñovero, E.T. Zellers, Microfabricated Gas Chromatograph for Rapid, Trace-Level Determinations of Gas-Phase Explosive Marker Compounds, Anal. Chem. 86 (2014) 655–663. https://doi.org/10.1021/ac402961t.

[3] I. Lara-Ibeas, C. Trocquet, R. Nasreddine, C. Andrikopoulou, V. Person, B. Cormerais, S. Englaro, S. Le Calvé, BTEX near real-time monitoring in two primary schools in La Rochelle, France, Air Qual Atmos Health. 11 (2018) 1091–1107. https://doi.org/10.1007/s11869-018-0611-3.

[4] A. Rodríguez-Cuevas, I. Lara-Ibeas, A. Leprince, M. Wolf, S. Le Calvé, Easy-to-manufacture micro gas preconcentrator integrated in a portable GC for enhanced trace detection of BTEX, Sensors and Actuators B: Chemical. 324 (2020) 128690. https://doi.org/10.1016/j.snb.2020.128690.

[5] J. Bryant-Genevier, E.T. Zellers, Toward a microfabricated preconcentrator-focuser for a wearable micro-scale gas chromatograph, Journal of Chromatography A. 1422 (2015) 299–309. https://doi.org/10.1016/j.chroma.2015.10.045.

[6] J. Wang, N. Nuñovero, R. Nidetz, S.J. Peterson, B.M. Brookover, W.H. Steinecker, E.T. Zellers, Belt-Mounted Micro-Gas-Chromatograph Prototype for Determining Personal Exposures to Volatile-Organic-Compound Mixture Components, Anal. Chem. 91 (2019) 4747–4754. https://doi.org/10.1021/acs.analchem.9b00263.

[7] A.M. Rydosz, D. Michon, K. Domanski, W. Maziarz, T. Pisarkiewicz, Various Preconcentrator Structures For Determination of Acetone in a Wide Range of Concentration, Advances in Electrical and Electronic Engineering. 14 (2016) 59-65–65. https://doi.org/10.15598/aeee.v14i1.1525.

[8] G. Gregis, J.-B. Sanchez, I. Bezverkhyy, W. Guy, F. Berger, V. Fierro, J.-P. Bellat, A. Celzard, Detection and quantification of lung cancer biomarkers by a micro-analytical device using a single metal oxide-based gas sensor, Sensors and Actuators B: Chemical. 255 (2018) 391–400. https://doi.org/10.1016/j.snb.2017.08.056.

[9] Directive 2008/50/EC of the European Parliament and of the Council of 21 May 2008 on ambient air quality and cleaner air for Europe, 2008. http://data.europa.eu/eli/dir/2008/50/oj/eng (accessed October 23, 2019).

[10] I. Lara-Ibeas, A. Rodríguez-Cuevas, C. Andrikopoulou, V. Person, L. Baldas, S. Colin, S. Le Calvé, Sub-ppb Level Detection of BTEX Gaseous Mixtures with a Compact Prototype GC Equipped with a Preconcentration Unit, Micromachines. 10 (2019) 187. https://doi.org/10.3390/mi10030187.

[11] J.-C. Soo, E.G. Lee, R.F. LeBouf, M.L. Kashon, W. Chisholm, M. Harper, Evaluation of a portable gas chromatograph with photoionization detector under variations of VOC concentration, temperature, and relative humidity, Journal of Occupational and Environmental Hygiene. 15 (2018) 351–360. https://doi.org/10.1080/15459624.2018.1426860.

[12] A. Garg, M. Akbar, E. Vejerano, S. Narayanan, L. Nazhandali, L.C. Marr, M. Agah, Zebra GC: A mini gas chromatography system for trace-level determination of hazardous air pollutants,

Sensors and Actuators B: Chemical. 212 (2015) 145–154. https://doi.org/10.1016/j.snb.2014.12.136.
[13] S. Zampolli, I. Elmi, F. Mancarella, P. Betti, E. Dalcanale, G.C. Cardinali, M. Severi, Real-time monitoring of sub-ppb concentrations of aromatic volatiles with a MEMS-enabled miniaturized gas-chromatograph, Sensors and Actuators B: Chemical. 141 (2009) 322–328. https://doi.org/10.1016/j.snb.2009.06.021.
[14] J. Yeom, C.R. Field, B. Bae, R.I. Masel, M.A. Shannon, The design, fabrication and characterization of a silicon microheater for an integrated MEMS gas preconcentrator, J. Micromech. Microeng. 18 (2008) 125001. https://doi.org/10.1088/0960-1317/18/12/125001.
[15] J. Lee, M. Zhou, H. Zhu, R. Nidetz, K. Kurabayashi, X. Fan, Fully Automated Portable Comprehensive 2-Dimensional Gas Chromatography Device, Anal. Chem. 88 (2016) 10266–10274. https://doi.org/10.1021/acs.analchem.6b03000.
[16] X. Huang, T. Bauder, T. Do, H. Suen, C. Boss, P. Kwon, J. Yeom, A Binder Jet Printed, Stainless Steel Preconcentrator as an In-Line Injector of Volatile Organic Compounds, Sensors. 19 (2019) 2748. https://doi.org/10.3390/s19122748.
[17] D.-W. You, Y.-S. Seon, Y. Jang, J. Bang, J.-S. Oh, K.-W. Jung, A portable gas chromatograph for real-time monitoring of aromatic volatile organic compounds in air samples, Journal of Chromatography A. 1625 (2020) 461267. https://doi.org/10.1016/j.chroma.2020.461267.
[18] K.M. Skog, F. Xiong, H. Kawashima, E. Doyle, R. Soto, D.R. Gentner, Compact, Automated, Inexpensive, and Field-Deployable Vacuum-Outlet Gas Chromatograph for Trace-Concentration Gas-Phase Organic Compounds, Anal. Chem. 91 (2019) 1318–1327. https://doi.org/10.1021/acs.analchem.8b03095.
[19] J. Sun, N. Xue, W. Wang, H. Wang, C. Liu, T. Ma, T. Li, T. Tan, Compact prototype GC-PID system integrated with micro PC and micro GC column, Journal of Micromechanics and Microengineering. 29 (2018) 29. https://doi.org/10.1088/1361-6439/aaf42c.
[20] J.W. Trzciński, R. Pinalli, N. Riboni, A. Pedrini, F. Bianchi, S. Zampolli, I. Elmi, C. Massera, F. Ugozzoli, E. Dalcanale, In Search of the Ultimate Benzene Sensor: The EtQxBox Solution, ACS Sensors. 2 (2017) 590–598. https://doi.org/10.1021/acssensors.7b00110.
[21] R.-S. Jian, Y.-S. Huang, S.-L. Lai, L.-Y. Sung, C.-J. Lu, Compact instrumentation of a μ-GC for real time analysis of sub-ppb VOC mixtures, Microchemical Journal. 108 (2013) 161–167. https://doi.org/10.1016/j.microc.2012.10.016.
[22] N.A. Zaidi, M.W. Tahir, M.J. Vellekoop, W. Lang, Design of Novel Ceramic Preconcentrator and Integration in Gas Chromatographic System for Detection of Ethylene Gas from Ripening Bananas, Sensors. 18 (2018) 2589. https://doi.org/10.3390/s18082589.
[23] T.-H. Tzeng, C.-Y. Kuo, S.-Y. Wang, P.-K. Huang, Y.-M. Huang, Y.-M. Huang, W.-C. Hsieh, Y.-J. Huang, P.-H. Kuo, S.-A. Yu, S.-C. Lee, Y.J. Tseng, W.-C. Tian, S.-S. Lu, A Portable Micro Gas Chromatography System for Lung Cancer Associated Volatile Organic Compound Detection, IEEE Journal of Solid-State Circuits. 51 (2016) 259–272. https://doi.org/10.1109/JSSC.2015.2489839.
[24] Y. Qin, Y.B. Gianchandani, A fully electronic microfabricated gas chromatograph with complementary capacitive detectors for indoor pollutants, Microsystems & Nanoengineering. 2 (2016) 15049. https://doi.org/10.1038/micronano.2015.49.
[25] H. Lahlou, J.-B. Sanchez, Y. Mohsen, X. Vilanova, F. Berger, E. Llobet, X. Correig, V. Fierro, A. Celzard, I. Gràcia, A planar micro-concentrator/injector for low power consumption microchromatographic analysis of benzene and 1, 3 butadiene, Microsystem Technologies. 18 (2012) 489–495.
[26] C. Zhan, M. Akbar, R. Hower, N. Nuñovero, J. A. Potkay, E. T. Zellers, A micro passive preconcentrator for micro gas chromatography, Analyst. (2020). https://doi.org/10.1039/D0AN01485K.
[27] T.H. Chappuis, B.A.P. Ho, M. Ceillier, F. Ricoul, M. Alessio, J.-F. Beche, C. Corne, G. Besson, J. Vial, D. Thiébaut, B. Bourlon, Miniaturization of breath sampling with silicon chip: application to volatile tobacco markers tracking, J. Breath Res. (2018). https://doi.org/10.1088/1752-7163/aad384.

[28] B. Han, H. Wang, H. Huang, T. Liu, G. Wu, J. Wang, Micro-fabricated packed metal gas preconcentrator for enhanced monitoring of ultralow concentration of isoprene, Journal of Chromatography A. (2018). https://doi.org/10.1016/j.chroma.2018.08.058.
[29] M.M. McCartney, Y. Zrodnikov, A.G. Fung, M.K. LeVasseur, J.M. Pedersen, K.O. Zamuruyev, A.A. Aksenov, N.J. Kenyon, C.E. Davis, An Easy to Manufacture Micro Gas Preconcentrator for Chemical Sensing Applications, ACS Sensors. 2 (2017) 1167–1174. https://doi.org/10.1021/acssensors.7b00289.
[30] S. Janssen, T. Tessmann, W. Lang, High sensitive and selective ethylene measurement by using a large-capacity-on-chip preconcentrator device, Sensors and Actuators B: Chemical. 197 (2014) 405–413. https://doi.org/10.1016/j.snb.2014.02.001.
[31] M. Leidinger, M. Rieger, T. Sauerwald, C. Alépée, A. Schütze, Integrated pre-concentrator gas sensor microsystem for ppb level benzene detection, Sensors and Actuators B: Chemical. 236 (2016) 988–996. https://doi.org/10.1016/j.snb.2016.04.064.
[32] M. Camara, P. Breuil, C. Pijolat, J.P. Viricelle, N.F. de Rooij, D. Briand, Tubular gas preconcentrators based on inkjet printed micro-hotplates on foil, Sensors and Actuators B: Chemical. 236 (2016) 1111–1117. https://doi.org/10.1016/j.snb.2016.06.121.
[33] T. Sukaew, H. Chang, G. Serrano, E.T. Zellers, Multi-stage preconcentrator/focuser module designed to enable trace level determinations of trichloroethylene in indoor air with a microfabricated gas chromatograph, Analyst. 136 (2011) 1664–1674. https://doi.org/10.1039/C0AN00780C.
[34] J. Lee, J. Lee, S.-H. Lim, Micro gas preconcentrator using metal organic framework embedded metal foam for detection of low-concentration volatile organic compounds, Journal of Hazardous Materials. 392 (2020) 122145. https://doi.org/10.1016/j.jhazmat.2020.122145.
[35] B. Zhao, F. Feng, X. Yang, F. Luo, H. Zhou, X. Li, Improved Performance of Micro-Preconcentrator Using Silicon Nanowires as a Surface Template, in: 2019 20th International Conference on Solid-State Sensors, Actuators and Microsystems Eurosensors XXXIII (TRANSDUCERS EUROSENSORS XXXIII), 2019: pp. 1281–1284. https://doi.org/10.1109/TRANSDUCERS.2019.8808319.
[36] J. Lee, S.-H. Lim, CNT Foam-Embedded Micro Gas Preconcentrator for Low-Concentration Ethane Measurements, Sensors (Basel). 18 (2018). https://doi.org/10.3390/s18051547.
[37] Y. Zhang, J. Sun, X. Zhu, J. Liu, Z. Ning, Mini pretreatment system integrated with micro pre-concentrator and micro GC column, Sensor Review. 37 (2017) 137–141. https://doi.org/10.1108/SR-09-2016-0154.
[38] C.-Y. Kuo, P.-S. Chen, H.-T. Chen, C.-J. Lu, W.-C. Tian, Development of micromachined preconcentrators and gas chromatographic separation columns by an electroless gold plating technology, J. Micromech. Microeng. 27 (2017) 035012. https://doi.org/10.1088/1361-6439/aa5aa3.
[39] F. Almazán, I. Pellejero, A. Morales, M.A. Urbiztondo, J. Sesé, M.P. Pina, Jesús Santamaría, Zeolite based microconcentrators for volatile organic compounds sensing at trace-level: fabrication and performance, J. Micromech. Microeng. 26 (2016) 084010. https://doi.org/10.1088/0960-1317/26/8/084010.
[40] X.F. Zhu, Z.W. Ning, J.H. Sun, T.J. Ma, Y.N. Zhang, J.H. Liu, Micro-Fabricated Pre-Concentrator Filled with Single-Walled Carbon Nanotubes as Adsorbent Material, Key Engineering Materials. 645–646 (2015) 681–686. https://doi.org/10.4028/www.scientific.net/KEM.645-646.681.
[41] M. Clément, S. Arzel, B. Le Bot, R. Seux, M. Millet, Adsorption/thermal desorption-GC/MS for the analysis of pesticides in the atmosphere, Chemosphere. 40 (2000) 49–56. https://doi.org/10.1016/S0045-6535(99)00230-1.
[42] T. Mokalled, J. Adjizian Gérard, M. Abboud, C. Trocquet, R. Nassreddine, V. Person, S. le Calvé, VOC tracers from aircraft activities at Beirut Rafic Hariri International Airport, Atmospheric Pollution Research. 10 (2019) 537–551. https://doi.org/10.1016/j.apr.2018.09.009.
[43] L. Tuduri, M. Millet, O. Briand, M. Montury, Passive air sampling of semi-volatile organic compounds, TrAC Trends in Analytical Chemistry. 31 (2012) 38–49. https://doi.org/10.1016/j.trac.2011.08.007.

[44] L. Vallecillos, A. Borrull, R.M. Marcé, F. Borrull, Passive sampling to control air quality in schools: Uptake rate determination and application, Indoor Air. 30 (2020) 1005–1017. https://doi.org/10.1111/ina.12684.
[45] M. Lévy, J. Al-Alam, C. Ridacker, S. Massemin, M. Millet, Use of XAD®-2 passive air samplers for monitoring environmental trends of PAHs, PCBs and pesticides in three different sites in Strasbourg and its vicinity (east of France), Atmospheric Environment. 195 (2018) 12–23. https://doi.org/10.1016/j.atmosenv.2018.09.052.
[46] G. Serrano, T. Sukaew, E.T. Zellers, Hybrid preconcentrator/focuser module for determinations of explosive marker compounds with a micro-scale gas chromatograph, Journal of Chromatography A. 1279 (2013) 76–85. https://doi.org/10.1016/j.chroma.2013.01.009.
[47] Y. Qin, Y.B. Gianchandani, iGC2 : an architecture for micro gas chromatographs utilizing integrated bi-directional pumps and multi-stage preconcentrators, J. Micromech. Microeng. 24 (2014) 065011. https://doi.org/10.1088/0960-1317/24/6/065011.
[48] A. Ghosh, C.R. Vilorio, A.R. Hawkins, M.L. Lee, Microchip gas chromatography columns, interfacing and performance, Talanta. 188 (2018) 463–492. https://doi.org/10.1016/j.talanta.2018.04.088.
[49] W.I. Wu, P. Rezai, H.H. Hsu, P.R. Selvaganapathy, Materials and methods for the microfabrication of microfluidic biomedical devices, in: X. (James) Li, Y. Zhou (Eds.), Microfluidic Devices for Biomedical Applications, Woodhead Publishing, 2013: pp. 3–62. https://doi.org/10.1533/9780857097040.1.3.
[50] M.A. Zareian-Jahromi, M. Ashraf-Khorassani, L.T. Taylor, M. Agah, Design, Modeling, and Fabrication of MEMS-Based Multicapillary Gas Chromatographic Columns, Journal of Microelectromechanical Systems. 18 (2009) 28–37. https://doi.org/10.1109/JMEMS.2008.2007267.
[51] T.H. Chappuis, B.A.P. Ho, M. Ceillier, F. Ricoul, M. Alessio, J.-F. Beche, C. Corne, G. Besson, J. Vial, D. Thiébaut, B. Bourlon, Miniaturization of breath sampling with silicon chip: application to volatile tobacco markers tracking, J. Breath Res. (2018). https://doi.org/10.1088/1752-7163/aad384.
[52] S. Zampolli, I. Elmi, G.C. Cardinali, L. Masini, F. Bonafè, F. Zardi, Compact-GC platform: A flexible system integration strategy for a completely microsystems-based gas-chromatograph, Sensors and Actuators B: Chemical. 305 (2020) 127444. https://doi.org/10.1016/j.snb.2019.127444.
[53] J. Wang, J. Bryant-Genevier, N. Nuñovero, C. Zhang, B. Kraay, C. Zhan, K. Scholten, R. Nidetz, S. Buggaveeti, E.T. Zellers, Compact prototype microfabricated gas chromatographic analyzer for autonomous determinations of VOC mixtures at typical workplace concentrations, Microsystems & Nanoengineering. 4 (2018) 17101. https://doi.org/10.1038/micronano.2017.101.
[54] C. Iliescu, H. Taylor, M. Avram, J. Miao, S. Franssila, A practical guide for the fabrication of microfluidic devices using glass and silicon, Biomicrofluidics. 6 (2012) 016505. https://doi.org/10.1063/1.3689939.
[55] Z. Cui, Wafer Bonding, in: D. Li (Ed.), Encyclopedia of Microfluidics and Nanofluidics, Springer US, Boston, MA, 2008: pp. 2179–2183. https://doi.org/10.1007/978-0-387-48998-8_1682.
[56] N.A. Zaidi, M.W. Tahir, M.J. Vellekoop, W. Lang, A Gas Chromatographic System for the Detection of Ethylene Gas Using Ambient Air as a Carrier Gas, Sensors. 17 (2017) 2283. https://doi.org/10.3390/s17102283.
[57] H. Lahlou, X. Vilanova, X. Correig, Gas phase micro-preconcentrators for benzene monitoring: A review, Sensors and Actuators B: Chemical. 176 (2013) 198–210. https://doi.org/10.1016/j.snb.2012.10.004.
[58] D. Michoń, A. Rydosz, K. Domański, W. Maziarz, T. Pisarkiewicz, Detection of acetone in exhaled breath with the use of micropreconcentrator and a commercial gas sensor, in: B. Swatowska, W. Maziarz, T. Pisarkiewicz, W. Kucewicz (Eds.), 2016: p. 1017511. https://doi.org/10.1117/12.2263268.

[59] M. Li, S. Biswas, M.H. Nantz, R.M. Higashi, X.-A. Fu, A microfabricated preconcentration device for breath analysis, Sensors and Actuators B: Chemical. 180 (2013) 130–136. https://doi.org/10.1016/j.snb.2012.07.034.
[60] E.H.M. Camara, P. Breuil, D. Briand, N.F. de Rooij, C. Pijolat, A micro gas preconcentrator with improved performance for pollution monitoring and explosives detection, Analytica Chimica Acta. 688 (2011) 175–182. https://doi.org/10.1016/j.aca.2010.12.039.
[61] B. Alfeeli, M. Agah, MEMS-Based Selective Preconcentration of Trace Level Breath Analytes, IEEE Sensors Journal. 9 (2009) 1068–1075. https://doi.org/10.1109/JSEN.2009.2025822.
[62] B. Alfeeli, H. Vereb, A. Dietrich, M. Agah, Low pressure drop micro preconcentrators with cobweb Tenax-TA film for analysis of human breath, in: 2011 IEEE 24th International Conference on Micro Electro Mechanical Systems, 2011: pp. 916–919. https://doi.org/10.1109/MEMSYS.2011.5734575.
[63] M. Akbar, M. Agah, A Microfabricated Propofol Trap for Breath-Based Anesthesia Depth Monitoring, J. Microelectromech. Syst. 22 (2013) 443–451. https://doi.org/10.1109/JMEMS.2012.2227949.
[64] B. Alfeeli, Chemical Micro Preconcentrators Development for Micro Gas Chromatography Systems, (2010). https://vtechworks.lib.vt.edu/handle/10919/29305 (accessed September 30, 2019).
[65] Y. Jang, J. Bang, Y.-S. Seon, D.-W. You, J.-S. Oh, K.-W. Jung, Carbon nanotube sponges as an enrichment material for aromatic volatile organic compounds, Journal of Chromatography A. 1617 (2020) 460840. https://doi.org/10.1016/j.chroma.2019.460840.
[66] A. Rydosz, W. Maziarz, T. Pisarkiewicz, K. Domański, P. Grabiec, A gas micropreconcentrator for low level acetone measurements, Microelectronics Reliability. 52 (2012) 2640–2646. https://doi.org/10.1016/j.microrel.2012.05.012.
[67] C.-J. Lu, E.T. Zellers, A dual-adsorbent preconcentrator for a portable indoor-VOC microsensor system, Analytical Chemistry. 73 (2001) 3449–3457.
[68] J. Lee, M. Jung, S. Barthwal, S. Lee, S.-H. Lim, MEMS gas preconcentrator filled with CNT foam for exhaled VOC gas detection, BioChip Journal. 9 (2015) 44–49. https://doi.org/10.1007/s13206-014-9106-y.
[69] B. Han, G. Wu, H. Wang, J. Wang, Micro-fabricated packed metal gas preconcentrator for low detection limit exhaled VOC gas measurements, in: IEEE, 2017: pp. 269–273. https://doi.org/10.1109/3M-NANO.2017.8286278.
[70] J. Wang, N. Nuñovero, Z. Lin, R. Nidetz, S. Buggaveeti, C. Zhan, K. Kurabayashi, W.H. Steinecker, E.T. Zellers, A Wearable MEMS Gas Chromatograph for Multi-Vapor Determinations, Procedia Engineering. 168 (2016) 1398–1401. https://doi.org/10.1016/j.proeng.2016.11.391.
[71] J. Wang, J. Ma, E.T. Zellers, Room-temperature-ionic-liquid coated graphitized carbons for selective preconcentration of polar vapors, Journal of Chromatography A. 1609 (2020) 460486. https://doi.org/10.1016/j.chroma.2019.460486.
[72] R. Huang, M. Lu, P. Wang, Y. Chen, J. Wu, M. Fu, L. Chen, D. Ye, Enhancement of the non-thermal plasma-catalytic system with different zeolites for toluene removal, RSC Adv. 5 (2015) 72113–72120. https://doi.org/10.1039/C5RA13604K.
[73] I. Lara-Ibeas, C. Megías-Sayago, A. Rodríguez-Cuevas, R. Ocampo-Torres, B. Louis, S. Colin, S. Le Calvé, Adsorbent screening for airborne BTEX analysis and removal, Journal of Environmental Chemical Engineering. (2019) 103563. https://doi.org/10.1016/j.jece.2019.103563.
[74] I. Lara-Ibeas, C. Megías-Sayago, B. Louis, S. Le Calvé, Adsorptive removal of gaseous formaldehyde at realistic concentrations, Journal of Environmental Chemical Engineering. 8 (2020) 103986. https://doi.org/10.1016/j.jece.2020.103986.
[75] X. Huang, Z. Huang, L. Zhang, R. Liu, Y. Lv, Highly efficient cataluminescence gas sensor for acetone vapor based on UIO-66 metal-organic frameworks as preconcentrator, Sensors and Actuators B: Chemical. 312 (2020) 127952. https://doi.org/10.1016/j.snb.2020.127952.
[76] M.-Y. Wong, W.-R. Cheng, M.-H. Liu, W.-C. Tian, C.-J. Lu, A preconcentrator chip employing μ-SPME array coated with in-situ-synthesized carbon adsorbent film for VOCs analysis, Talanta. 101 (2012) 307–313. https://doi.org/10.1016/j.talanta.2012.09.031.

[77] E.H.M. Camara, Développement d'un micro-préconcentrateur pour la détection de substances chimiques à l'état de trace en phase gaz, (2009). https://tel.archives-ouvertes.fr/tel-00448980 (accessed October 11, 2019).
[78] R. Kalidoss, S. Umapathy, An overview on the exponential growth of non-invasive diagnosis of diabetes mellitus from exhaled breath by nanostructured metal oxide Chemi-resistive gas sensors and μ-preconcentrator, Biomed Microdevices. 22 (2020) 2. https://doi.org/10.1007/s10544-019-0448-z.
[79] V. Gold, ed., The IUPAC Compendium of Chemical Terminology: The Gold Book, 4th ed., International Union of Pure and Applied Chemistry (IUPAC), Research Triangle Park, NC, 2019. https://doi.org/10.1351/goldbook.
[80] M.P. Tsakas, A.P. Siskos, P. Siskos, Indoor Air Pollutants and the Impact on Human Health, Chemistry, Emission Control, Radioactive Pollution and Indoor Air Quality. (2011). https://doi.org/10.5772/18806.
[81] F. Ahmed, S. Hossain, S. Hossain, A.N.M. Fakhruddin, A.T.M. Abdullah, M.A.Z. Chowdhury, S.H. Gan, Impact of household air pollution on human health: source identification and systematic management approach, SN Appl. Sci. 1 (2019) 418. https://doi.org/10.1007/s42452-019-0405-8.
[82] M. Akbar, M. Restaino, M. Agah, Chip-scale gas chromatography: From injection through detection, Microsystems & Nanoengineering. 1 (2015) 15039. https://doi.org/10.1038/micronano.2015.39.
[83] G. Coelho Rezende, S. Le Calvé, J.J. Brandner, D. Newport, Micro photoionization detectors, Sensors and Actuators B: Chemical. 287 (2019) 86–94. https://doi.org/10.1016/j.snb.2019.01.072.
[84] M.P. Van der Schee, N. Fens, P. Brinkman, L.D.J. Bos, M.D. Angelo, T.M.E. Nijsen, R. Raabe, H.H. Knobel, T.J. Vink, P.J. Sterk, Effect of transportation and storage using sorbent tubes of exhaled breath samples on diagnostic accuracy of electronic nose analysis, Journal of Breath Research. 7 (2012) 016002.
[85] I. Horváth, P.J. Barnes, S. Loukides, P.J. Sterk, M. Högman, A.-C. Olin, A. Amann, B. Antus, E. Baraldi, A. Bikov, A European Respiratory Society technical standard: exhaled biomarkers in lung disease, European Respiratory Journal. 49 (2017) 1600965.